AD-A059 717 DYNAMICS TECHNOLOGY INC TORRANCE CALIF* F/G 20/4
ANALYTICAL PREDICTIONS OF BOUNDARY-LAYER TRANSITION IN A HEATED--ETC(U)
JUN 78 K T TZOU N00014-77-C-0005
UNCLASSIFIED DT-7802-2A NL

| OF |
AD
A059717

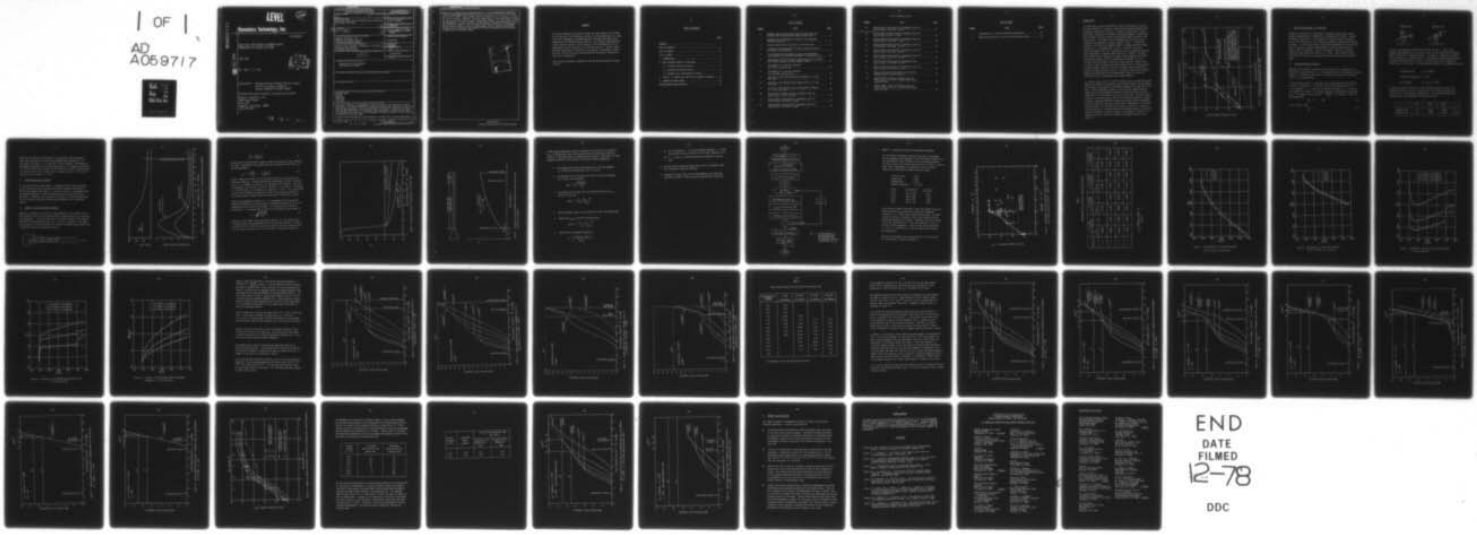

END
DATE
FILMED
12-78
DDC

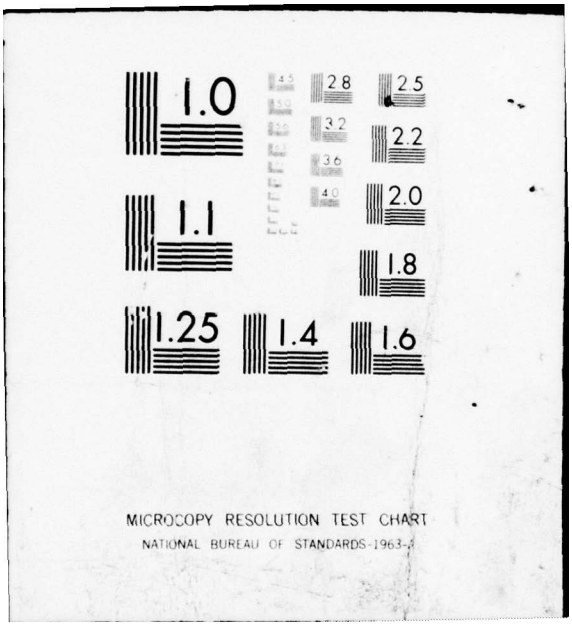
1.0
1.1
1.25
1.4
1.6
2.0
2.2
2.5
2.8
3.2
3.6
4.0
MICROCOPY RESOLUTION TEST CHART
NATIONAL BUREAU OF STANDARDS-1963-A

LEVEL II

12

Dynamics Technology, Inc.

DT-7802-2A

ANALYTICAL PREDICTIONS OF BOUNDARY-LAYER TRANSITION IN A HEATED FLOW TUBE

JUNE 1978

BY: KENT T. S. TZOU

SUPPORTED BY: DEFENSE ADVANCED RESEARCH PROJECTS AGENCY
AND OFFICE OF NAVAL RESEARCH
CONTRACT N00014-77-C-0005 (P0002)

DYNAMICS TECHNOLOGY, INC.
3838 CARSON STREET
SUITE 110
TORRANCE, CALIFORNIA 90503
(213) 540-5557

UNCLASSIFIED

SECURITY CLASSIFICATION OF THIS PAGE (When Data Entered)

REPORT DOCUMENTATION PAGE		READ INSTRUCTIONS BEFORE COMPLETING FORM
1. REPORT NUMBER (6)	2. GOVT ACCESSION NO.	3. RECIPIENT'S CATALOG NUMBER (9)
4. TITLE (and Subtitle) Analytical Predictions of Boundary-Layer Transition In A Heated Flow Tube,		5. TYPE OF REPORT & PERIOD COVERED Technical Report,
		6. PERFORMING ORG. REPORT NUMBER (14) DT-7802-2A
7. AUTHOR(s) (10) Kent T. S. Tzou		8. CONTRACT OR GRANT NUMBER(s) (15) Contract N00014-77-C-0005 (P0002)
9. PERFORMING ORGANIZATION NAME AND ADDRESS Dynamics Technology, Inc. 3838 Carson Street, Suite 110 Torrance, California 90503		10. PROGRAM ELEMENT, PROJECT, TASK AREA & WORK UNIT NUMBERS NR 062-565
11. CONTROLLING OFFICE NAME AND ADDRESS Office of Naval Research, Department of the Navy (11) 800 North Quincy Street Arlington, Virginia 22217		12. REPORT DATE June 1978
		13. NUMBER OF PAGES 46
14. MONITORING AGENCY NAME & ADDRESS(if different from Controlling Office) (12) 51p.		15. SECURITY CLASS. (of this report) UNCLASSIFIED
		15a. DECLASSIFICATION/DOWNGRADING SCHEDULE

16. DISTRIBUTION STATEMENT (of this Report)

Approved for Public Release;
Distribution Unlimited.

17. DISTRIBUTION STATEMENT (of the abstract entered in Block 20, if different from Report)

18. SUPPLEMENTARY NOTES

19. KEY WORDS (Continue on reverse side if necessary and identify by block number)

Boundary layer
Heating
Stability
Transition
Flow Tube

20. ABSTRACT (Continue on reverse side if necessary and identify by block number)

This report documents a complementary analytical study to the Colorado flow-tube experiments. An improved method for analyzing boundary-layer transition in the flow tube has been developed. The method includes the effects of transverse curvature and upstream contraction on the boundary-layer development, coupled with an iterative technique to account for the displacement thickness correction to the pressure distribution in the flow tube.

A series of calculations has been performed to simulate the flow-tube experiment, a

DD FORM 1473 (FACSIMILE)

393 137

78 10 02 095 LB

UNCLASSIFIED

SECURITY CLASSIFICATION OF THIS PAGE (When Data Entered)

heated test section with one unheated section. At the experimental transition location, the computed amplification factors vary from $e^{11.6}$ to $e^{15.8}$ with a mean value of $e^{14.0}$ which is much higher than the traditional "e^{9}" criterion. Based on the "e^{14}" criterion, reasonably favorable comparisons with the experimental results are obtained with this more accurate computation scheme. The calculations provide the explanation, at least partially, of the apparent reduced effectiveness of surface heating at large ΔT. The explanation rests upon the role of the unheated section and the effects unique to a tube boundary layer. Further calculations indicate that a significant improvement of the tube performance may be obtained by heating of the extension tube.

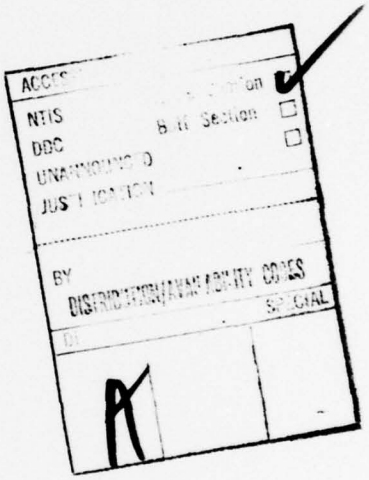

FOREWORD

This report documents an analytical effort for the estimate of the effect of wall heating on the transition location of the boundary layer in a tube. This effort complements the DARPA-sponsored flow-tube experiment being conducted at the Colorado State University. The findings reported herein clearly identify several critical aspects of the interpretation of the experimental results acquired in the flow-tube facility. Several rather favorable comparisons, in contrast to the apparent discrepancies cited in the past, with the test data are obtained when the present findings are taken into consideration.

This work was sponsored by DARPA/TTO under ONR Contract N00014-77-C-0005 (P0002).

TABLE OF CONTENTS

LIST OF FIGURES

List of Figures, Cont'd.

LIST OF TABLES

1. INTRODUCTION

In recent years, several experimental efforts have focused on the use of surface heating as a means of stabilizing the laminar boundary layer adjoining a body moving in water. In order to obtain data in a more controlled, steady-state environment, Autonetics/Rockwell International has initiated a series of tests at the Colorado State University flow-tube facility. The primary results obtained from this series of experiments are summarized in Figure 1 (Barker, 1977). A substantial increase in the transition Reynolds number is evident when the surface overheat, ΔT, is increased from 0 to $5^{o}C$. Above $5^{o}C$, the effect of heating appears to be less consequential and the transition Reynolds number approaches an apparent upper limit of $R_t = 42 \times 10^6$. The theoretical predictions of Wazzan et al (1968, 1970) suggested that transition Reynolds numbers of up to 200×16^6 may be possible in a zero pressure gradient boundary layer with surface heating. Dashed lines in Figure 1 show the results from those predictions for a zero pressure gradient boundary layer (β=0) and for a boundary layer subjected to a favorable pressure gradient (β=0.07). The rather significant disparity between the predictions and the experimental results has been the primary cause for numerous experimental modifications.

In a recent study, Tzou et al (1977) indicated that the noted discrepancy between the theoretical predictions and the experimental results might be attributable to the geometric differences between a flow tube and a flat plate. These conjectures, however, must be further substantiated by comparison of the experimental findings with more accurate analytical predictions of the transition location in a flow tube. The main features unique to a flow-tube system, such as the effects of transverse surface curvature, upstream contraction section and boundary-layer displacement thickness, should be included in these "exact" computations. These main features unique to a flow-tube are discussed in Section 2. Results of the calculations for a heated tube with an unheated extension, using this improved theoretical prediction method, are presented in Section 3. A summary and several conclusions based on the present results are in Section 4.

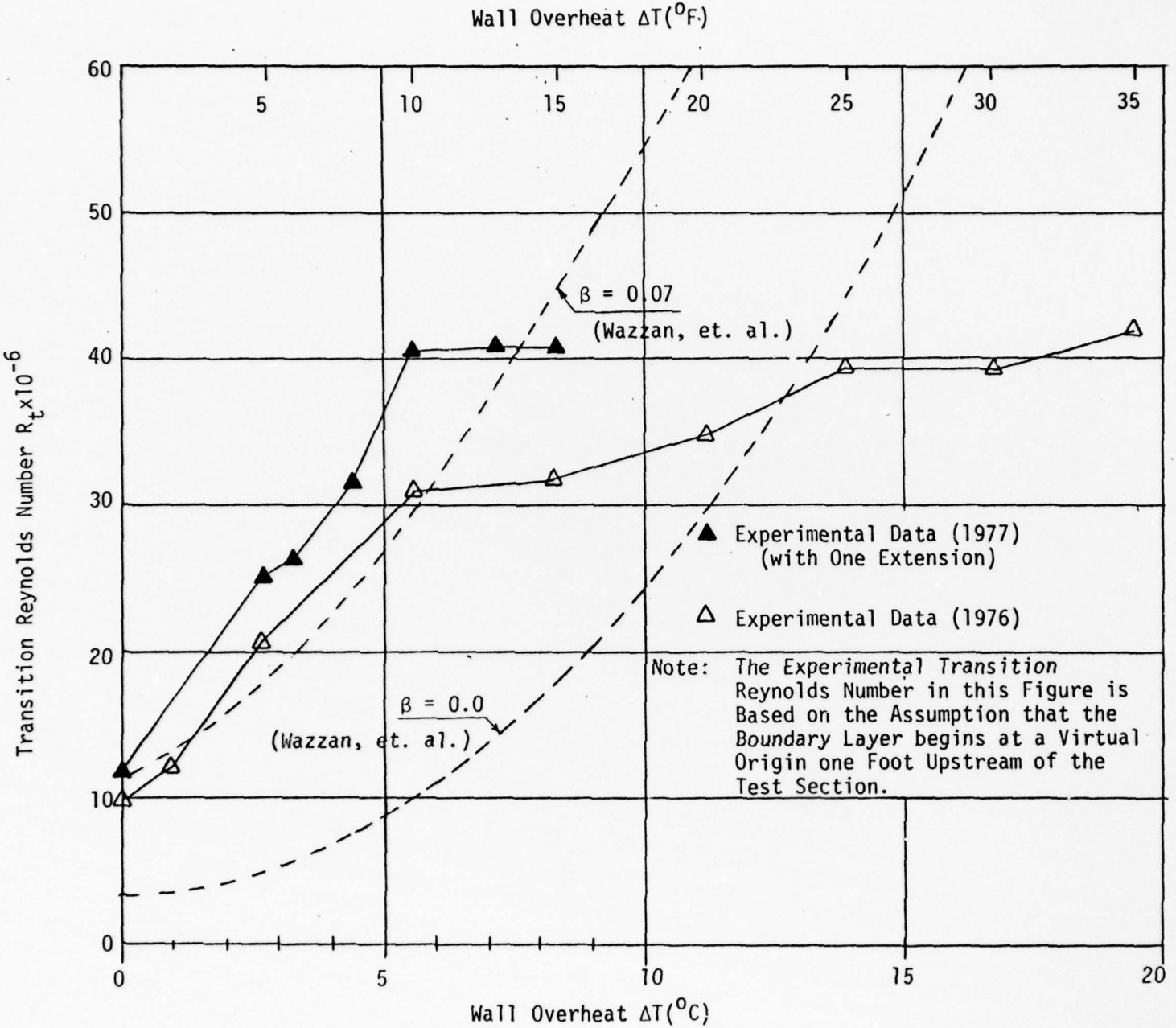

Figure 1. Boundary Layer Transition Data and Predictions for the Colorado Flow Tube Experiment (Barker, 1976, 1977)

2. MAIN FEATURES UNIQUE TO A FLOW TUBE

A complete simulation of a hydrodynamic phenomenon requires that the two systems be geometrically, kinematically, and dynamically similar. Because of physical constraints, it is impossible to achieve an exact simulation of the flow field around a given external axisymmetric body with an internal flow-tube. In order to be able to utilize the experimental results obtained from a flow tube, a thorough understanding of the flow characteristics within a tube is essential. Several key elements unique to a flow-tube system have been identified (Tzou et. al., 1977). These elements need to be included for more accurate computations and they are briefly discussed below.

2.1 Transverse Surface Curvature

Generally, the effect of transverse surface curvature is important only if the boundary layer thickness, δ, is not negligibly small as compared to the body radius r_o. Furthermore, the effect is different for internal and external flows as is discussed below.

In the following sketch "r" represents the distance measured from the body axis and is related to "r_o", the local radius of the body surface (i.e., $y = 0$) through $r = r_o + y\cos\alpha$ for an external flow and $r = r_o - y\cos\alpha$ for an internal flow, where α is the angle that the surface makes with the body axis. A transverse curvature term, $t = \frac{y \cos \alpha}{r_o}$, is introduced. Then, for an external flow:

$$\frac{r}{r_o} = 1 + t \,, \quad \text{and} \tag{1}$$

for an internal flow:

$$\frac{r}{r_o} = 1 - t. \tag{2}$$

EXTERNAL FLOW

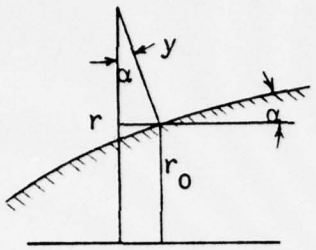

INTERNAL FLOW

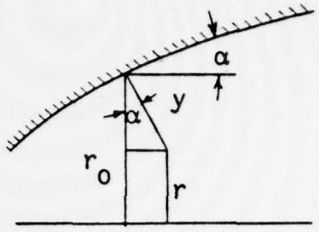

In order to investigate the quantitative effect of this t term in the boundary-layer equations for an internal flow, the TAPS Code (Gentry & Wazzan, 1976) is modified to include the effect. The effect of transverse curvature on the evolution of a boundary-layer is illustrated by considering the Rockwell/ Autonetics flow-tube which is circular in cross section with a diameter of 10.16 cm and is 6.10 m long. The flow conditions used for this demonstration are:

freestream speed $U_o = 6.10 m/sec$

freestream temperature $T_\infty = 10^oC$

wall overheat $\Delta T = T_w - T_\infty = 5.56^oC.$

In order to isolate the effects of the transverse surface curvature, the pressure coefficient, $C_p(X)$, is assumed to be zero for both the internal flow as well as the equivalent external flow. The computed boundary-layer characteristics are presented in the following table.

	X(m)	δ(mm)	θ(mm)	H
Internal Flow	6.10	5.6541	0.6909	2.72
External Flow	6.10	5.6616	0.7874	2.40

Note that the effect of flow geometry on the boundary-layer thickness is quite small even when the ratio of the boundary-layer thickness, δ, to the radius of the tube, r_o, is about 0.11 at this location. The effect on the momentum thickness, θ, and the shape factor, H, is, however, significant. It is also interesting to reveal that the transverse surface curvature causes an internal flow to have a higher value of shape factor (H = 2.72) than its external flow counterpart (H = 2.40).

2.2 Upstream Contraction Section

In the cited flow-tube experiments, a contraction section exists upstream of the flow tube in order to reduce the 60.96cm diameter supply pipe to the 10.16cm diameter test section. As shown in Figure 2, the boundary-layer displacement thickness in the contraction section varies with the flow conditions. Therefore, for an accurate calculation of the flow characteristics in the tube, calculations should begin upstream of the contraction section.

2.3 Boundary Layer Displacement Thickness

Because of the physical constraint of the boundaries in an internal flow, a much stronger effect on the freestream flow is expected than for its external flow counterpart. Since the flow rate Q is constant along the flow tube but the effective cross-sectional area, $\pi r^2 = \pi(r_o - \delta^*)^2$, decreases in the downstream direction (see sketch below) as a result of boundary-layer growth, the "freestream" speed must change according to:

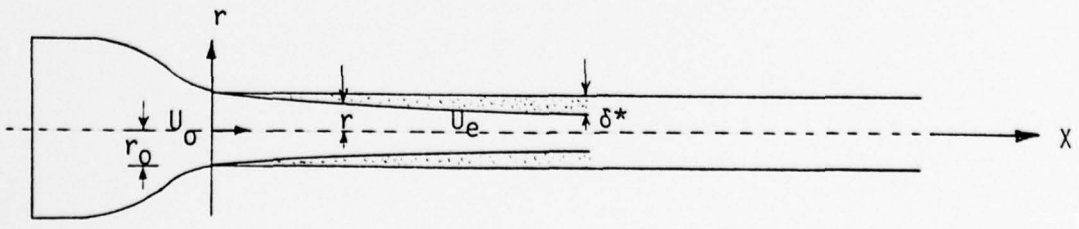

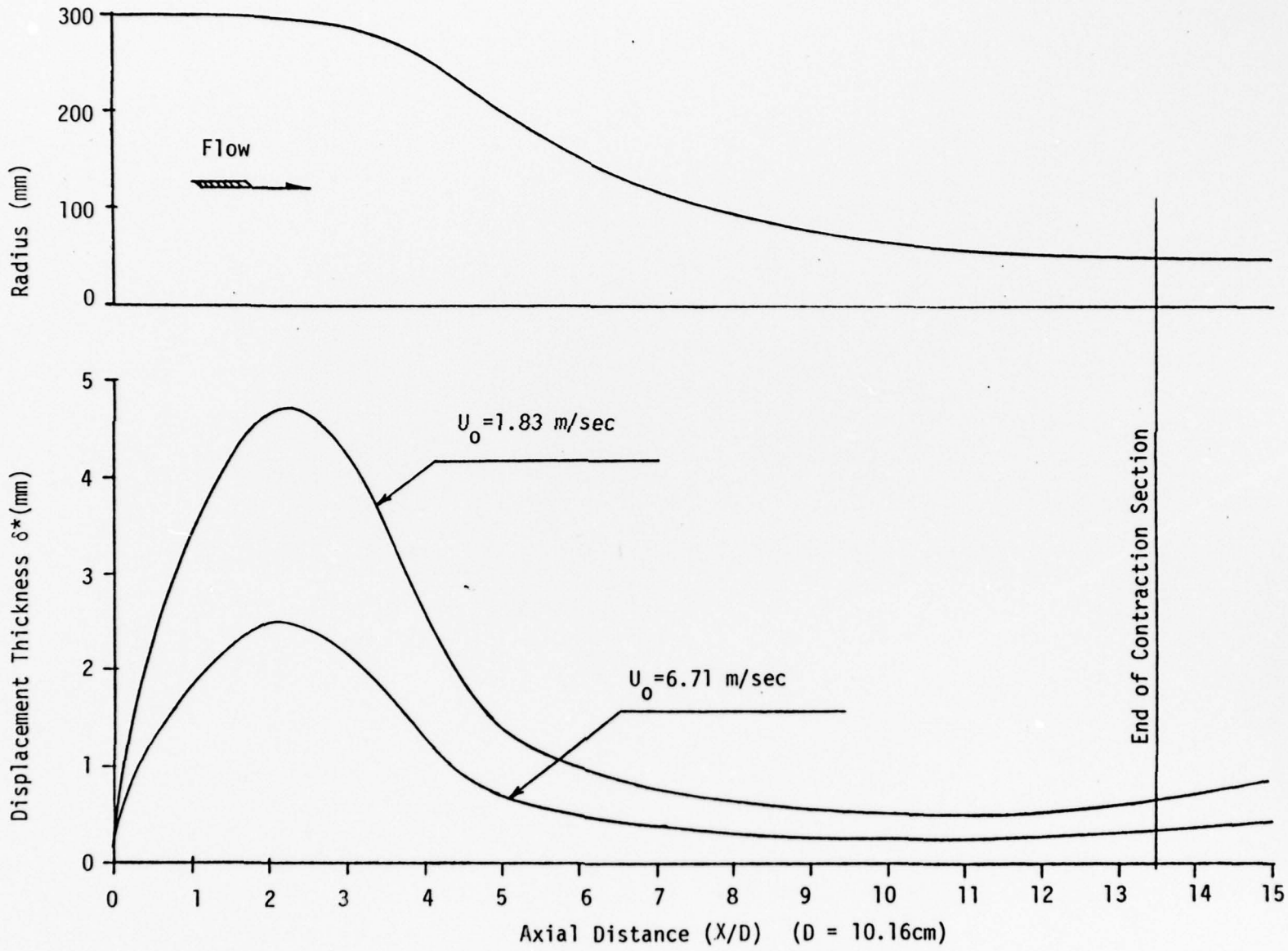

Figure 2. Boundary-Layer Displacement Thickness in the Upstream Contraction Section

$$\frac{U_e}{U_o} = \left(\frac{r_o}{r_o-\delta^*}\right)^2 . \qquad (3)$$

We note that, for the present purposes, simple one-dimensional flow relations are used. The effect of this speed change on the pressure coefficient, C_p, can be expressed as

$$C_p = 1 - \left(\frac{U_e}{U_o}\right)^2 = 1 - \left[\frac{r_o}{r_o-\delta^*}\right]^4 . \qquad (4)$$

Figure 3 shows the variation of C_p along the Autonetics flow-tube for two different conditions. Without applying the displacement thickness correction on C_p, it is customary to assume $C_p = 0$ throughout the flow-tube. With such a correction, C_p at the end of a 6.10m flow tube is -0.13 when U_o = 6.71m/sec, $\Delta T = 16.67^oC$ and C_p is -0.27 when U_o = 1.83m/sec, $\Delta T = 0^oC$. It is significant to note that the general assumption of either a zero pressure gradient or a constant pressure gradient flow within the tube is definitely incorrect.

Since the displacement thickness, δ^*, is a consequence of the particular pressure distribution in the flow-tube, an accurate estimation of δ^* can be obtained only by an iterative procedure. To initiate such an iterative calculation, it is assumed that δ^* can be first estimated by (See Figure 4)

$$\delta^* = C\sqrt{\frac{\nu(X-X_o+A)}{U_o}} \qquad (5)$$

where X_o is the length of the contraction section, A is the distance from a virtual origin to the beginning of the flow tube test section. It should be noted that this simplification was only used to start the computation and that the actual calculation of $\delta^*(X)$ was used for subsequent iterations.

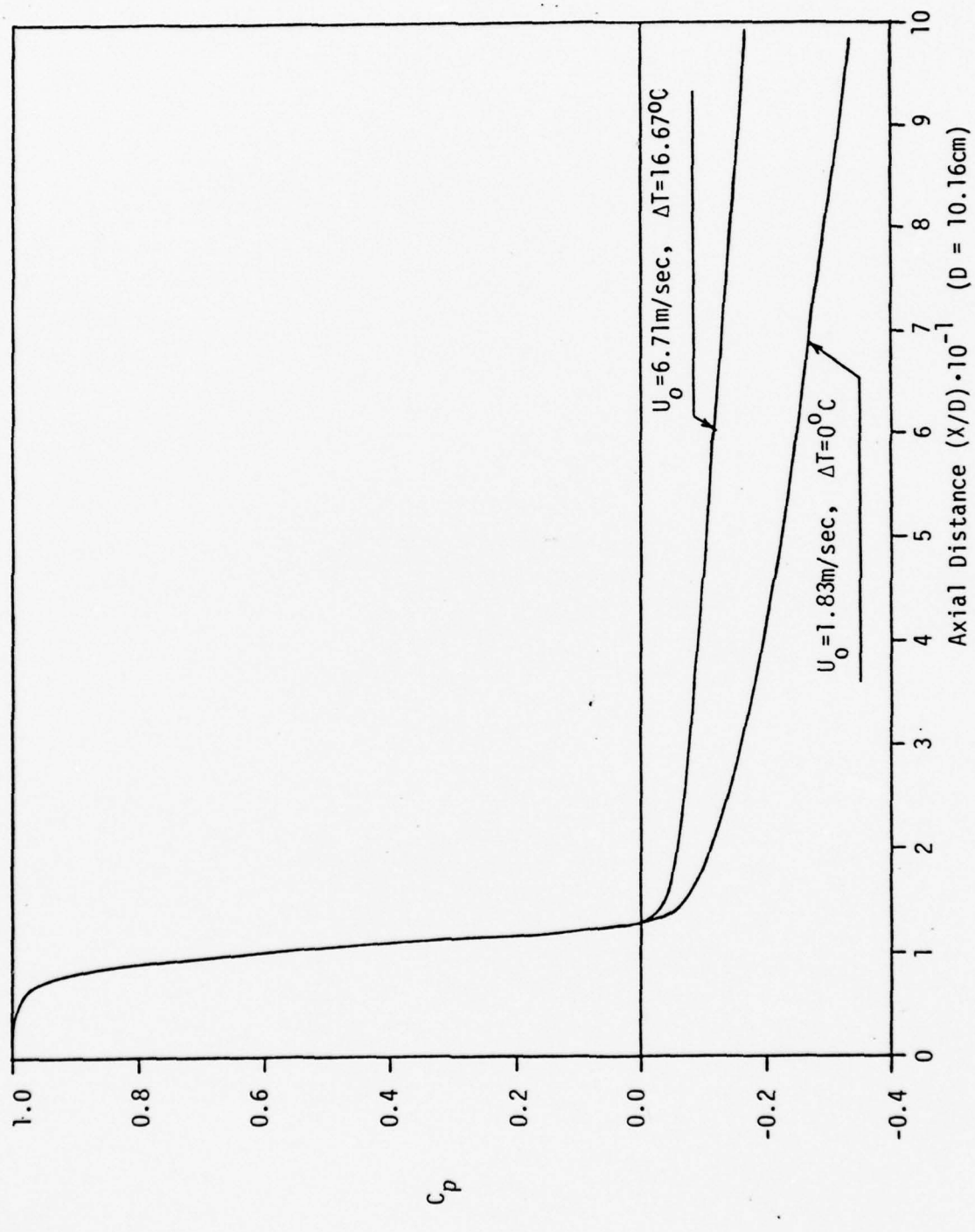

Figure 3. Pressure Coefficient Distribution in the Flow Tube

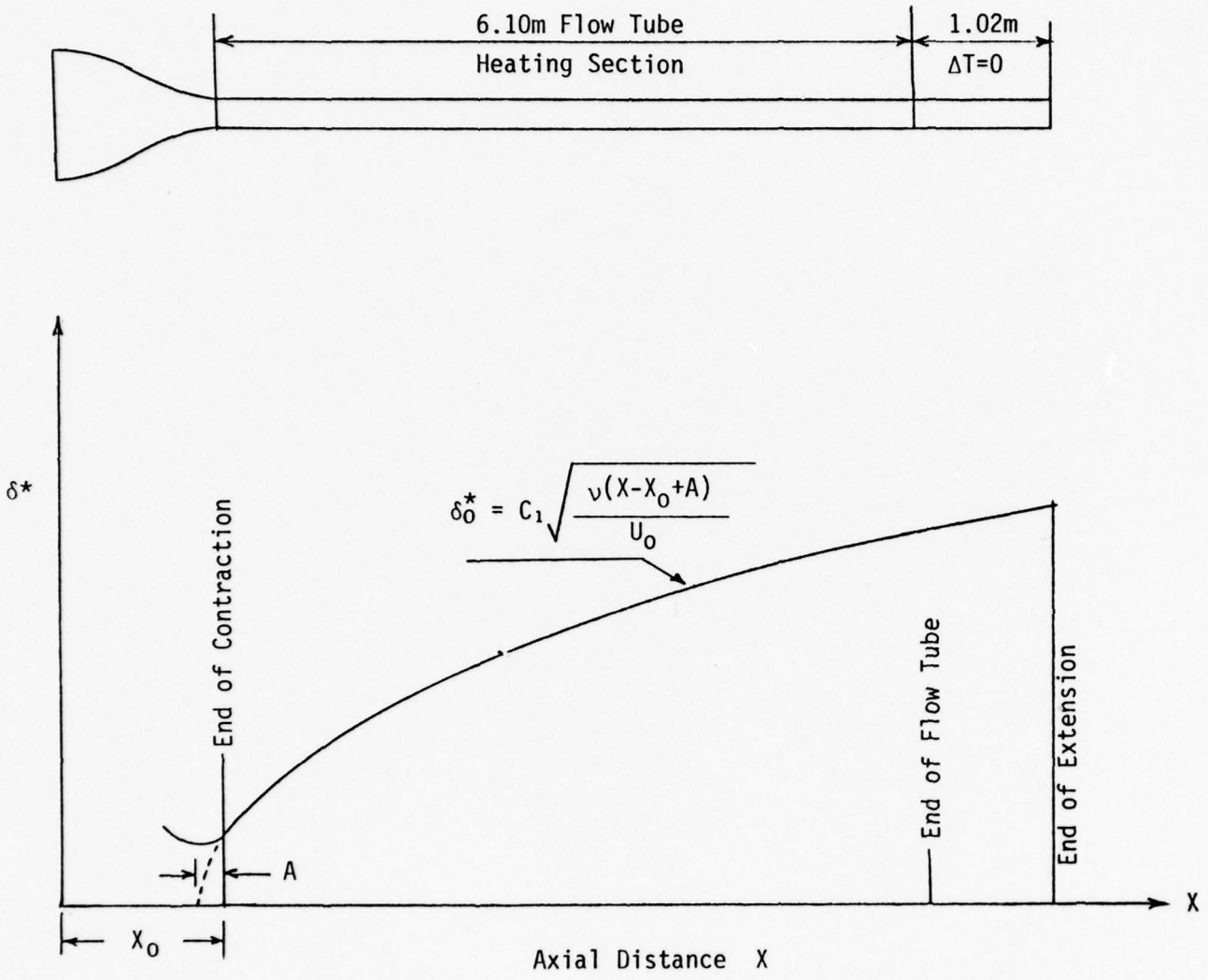

Figure 4. A Sketch of the Displacement Thickness Variation Input to the Iterative Calculation

A flow diagram showing the iterative procedure to account for δ^* correction on C_p in the boundary layer flow calculation and the subsequent stability analysis is described below in conjunction with Figure 5. Note that all three features discussed in the section are included in these computations.

1. The computation requires input data such as the tube geometry X, r_o and the flow conditions U_o, ΔT, T_∞ and ν.

2. Use equation (5) to calculate the initial δ^* value by assuming $C_1=1.5$, $X_o=1.37m$ and $A=0.27m$

$$\delta^*_{(o)} = C_1 \sqrt{\frac{\nu(X-X_o+A)}{U_o}}$$

3. Use equation (4) to obtain the corresponding variation of C_p along the flow tube

$$C_{p(1)} = 1 - \left[\frac{r_o}{r_o - \delta^*_{(o)}} \right]^4$$

4. Perform Boundary layer flow calculation to obtain calculated $\delta^*_{(i)}$

5. Compute new $C_{p(i+1)}$ from the calculated $\delta^*_{(i)}$

$$C_{p(i+1)} = 1 - \left[\frac{r_o}{r_o - \delta^*_{(i)}} \right]^4$$

6. Calculate the convergence parameter ε_i

$$\varepsilon_i = \left[\frac{C_{p(i+1)} - C_{p(i)}}{C_{p(i+1)}} \right]$$

7. (a) If the iteration $i < 3$ or the convergence parameter $\varepsilon_i > 0.005$, the procedure return to step (4) for the next iteration (i+1).

   (b) If $i \geq 3$ and $\varepsilon_i \leq 0.005$ the calculation proceed to the next step.

8. Perform stability analysis based on the results of boundary layer flow calculation from last iteration.

9. Determine the $\text{Log}_e\ (A/A_o)$ for the corresponding flow conditions specified in step (1) from the spatial amplification factor map.

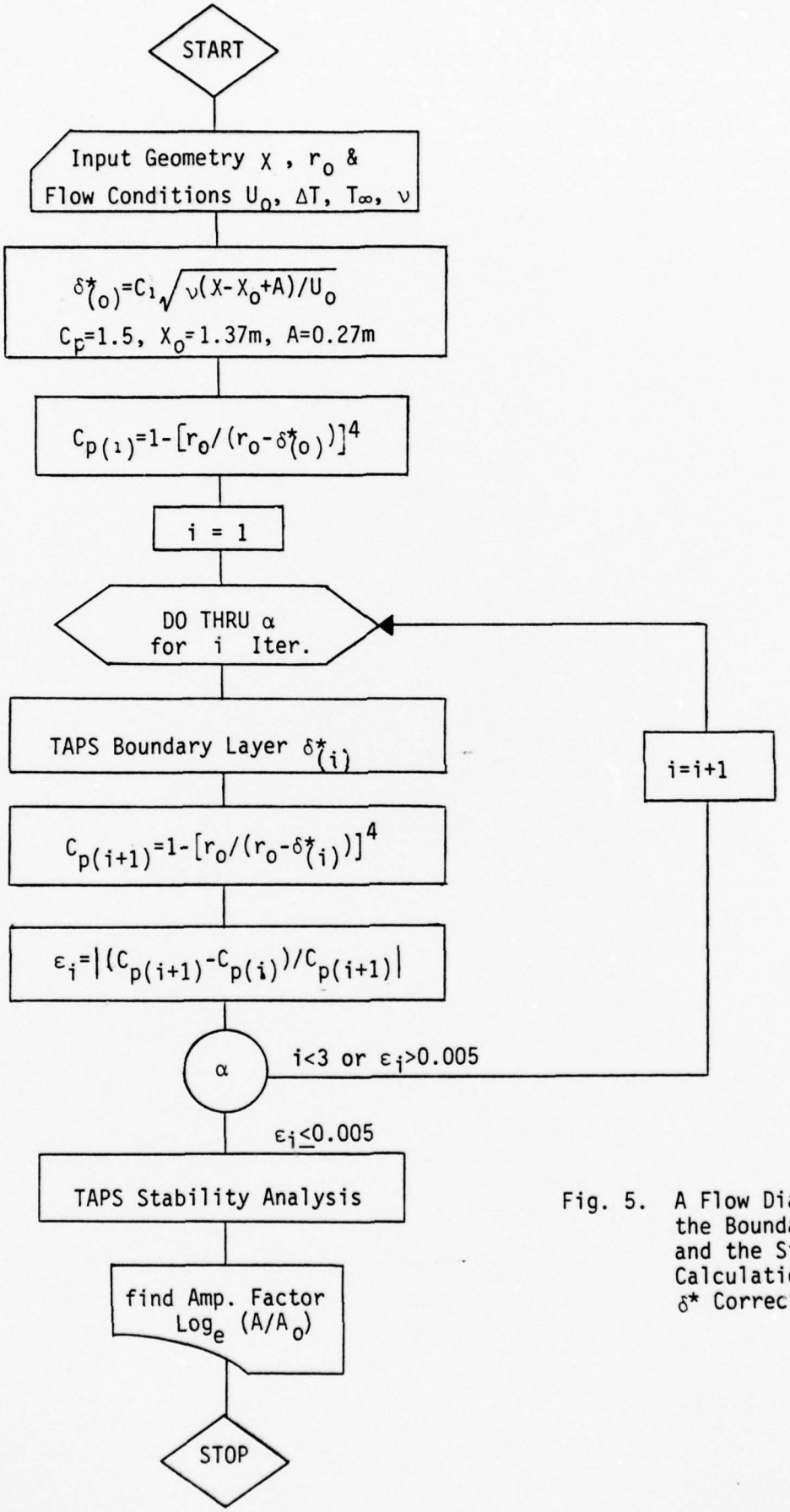

Fig. 5. A Flow Diagram for the Boundary Layer and the Stability Calculations Including δ* Correction on C_p.

3. RESULTS - A HEATED FLOW TUBE WITH AN UNHEATED EXTENSION

All the effects discussed in Section 2 have been incorporated into the boundary-layer component of the TAPS Code to compare with the experimental results obtained with one unheated extension tube and a laminar flow nozzle that are shown in Figure 6. Four of these "best" experimental flow conditions (solid circles in Figure 6) are selected for further analytical study.

Flow Tube Inlet	:	1.37m
Heated Tube	:	6.10m
Unheated Tube	:	1.22m
Ambient Temperature	:	T_∞ = 10°C

ΔT(°C)	R_t (Figure 6)	U_o (m/sec)
0.00	12.0×10^6	2.06
2.78	25.0×10^6	4.29
5.56	40.0×10^6	6.86
8.33	40.3×10^6	6.89

Following the procedure described in the flow diagram (Figure 5), three iterations were required to satisfy the convergence criterion of $\varepsilon_i \leq 0.005$ for the four selective cases. As shown in Table 1 and also in Figures 7 and 8, the iteration of the calculation converge very rapidly. Therefore, the initial selection of the coefficients C_1, A and X_o in equation 5 is not so critical in the computation. In this study, same coefficients C_1 = 1.50, A = 0.27m and X_o = 1.37m are used for initiating the calculations.

Variations of boundary-layer characteristics in the flow tube are illustrated in Figures 9 through 11.

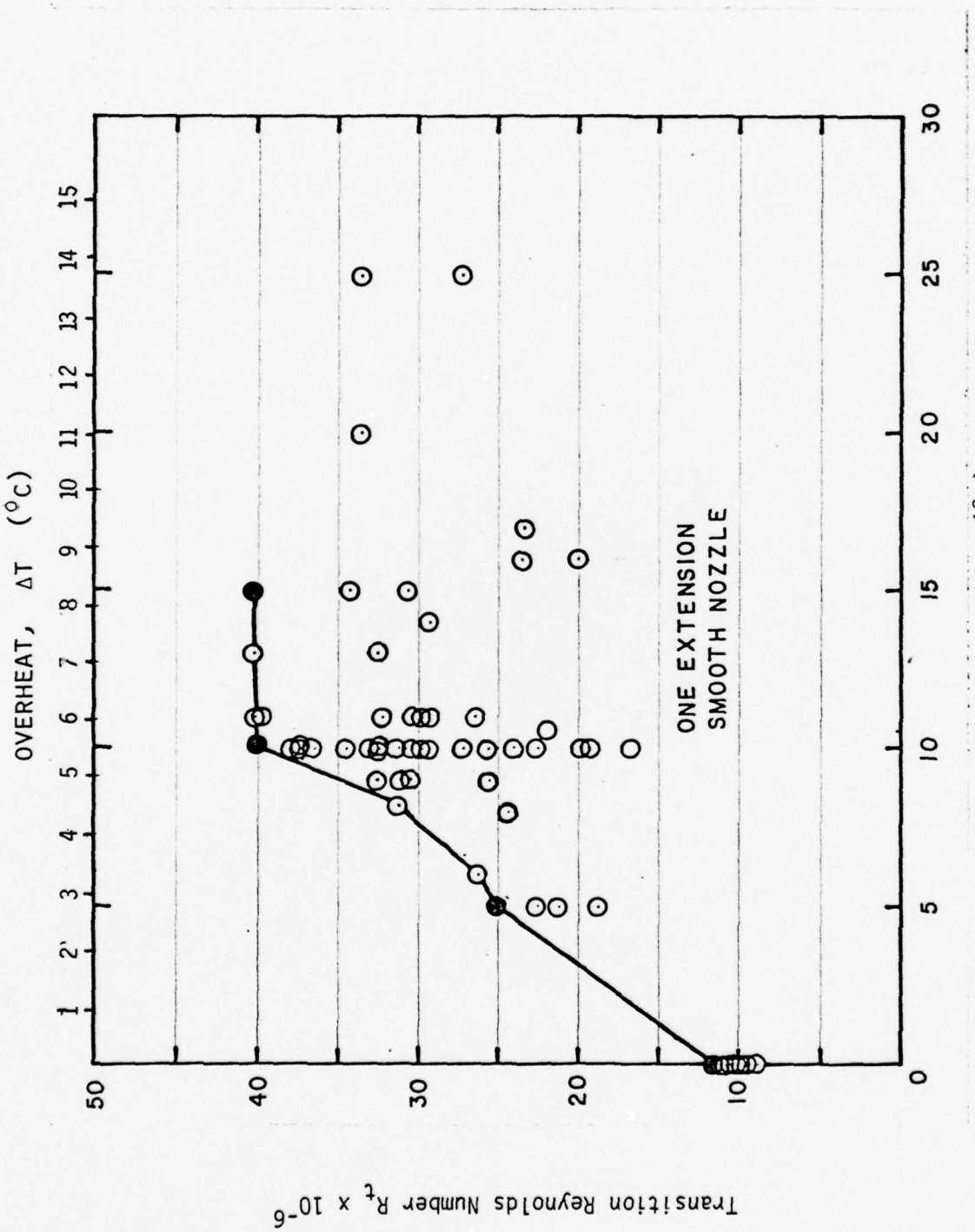

Figure 6. Experimental Transition Reynolds number data showing scatter due to water quality variation. (Barker, 1978.)

TABLE 1

Convergence of C_p from the Iterative Calculations

Iteration	$\Delta T = 0^oC$, $U_o = 2.06$ m/sec		$\Delta T = 2.78^oC$, $U_o = 4.29$ m/sec		$\Delta T = 5.56^oC$, $U_o = 6.86$ m/sec		$\Delta T = 8.33^oC$, $U_o = 6.89$ m/sec	
	$C_{p(i+1)}$	ε_i	$C_{p(i+1)}$	ε_i	$C_{p(i+1)}$	ε_i	$C_{p(i+1)}$	ε_i
i = 0	-0.2856	-	-0.1921	-	-0.1498	-	-0.1492	-
i = 1	-0.2888	0.0111	-0.2010	0.0443	-0.1581	0.0525	-0.1555	0.0405
i = 2	-0.2919	0.0106	-0.2005	0.0025	-0.1572	0.0057	-0.1546	0.0058
i = 3	-0.2905	0.0048	-0.2006	0.0005	-0.1574	0.0013	-0.1547	0.0006

$$\varepsilon_i = \left| \frac{C_{p(i+1)} - C_{p(i)}}{C_{p(i+1)}} \right|$$

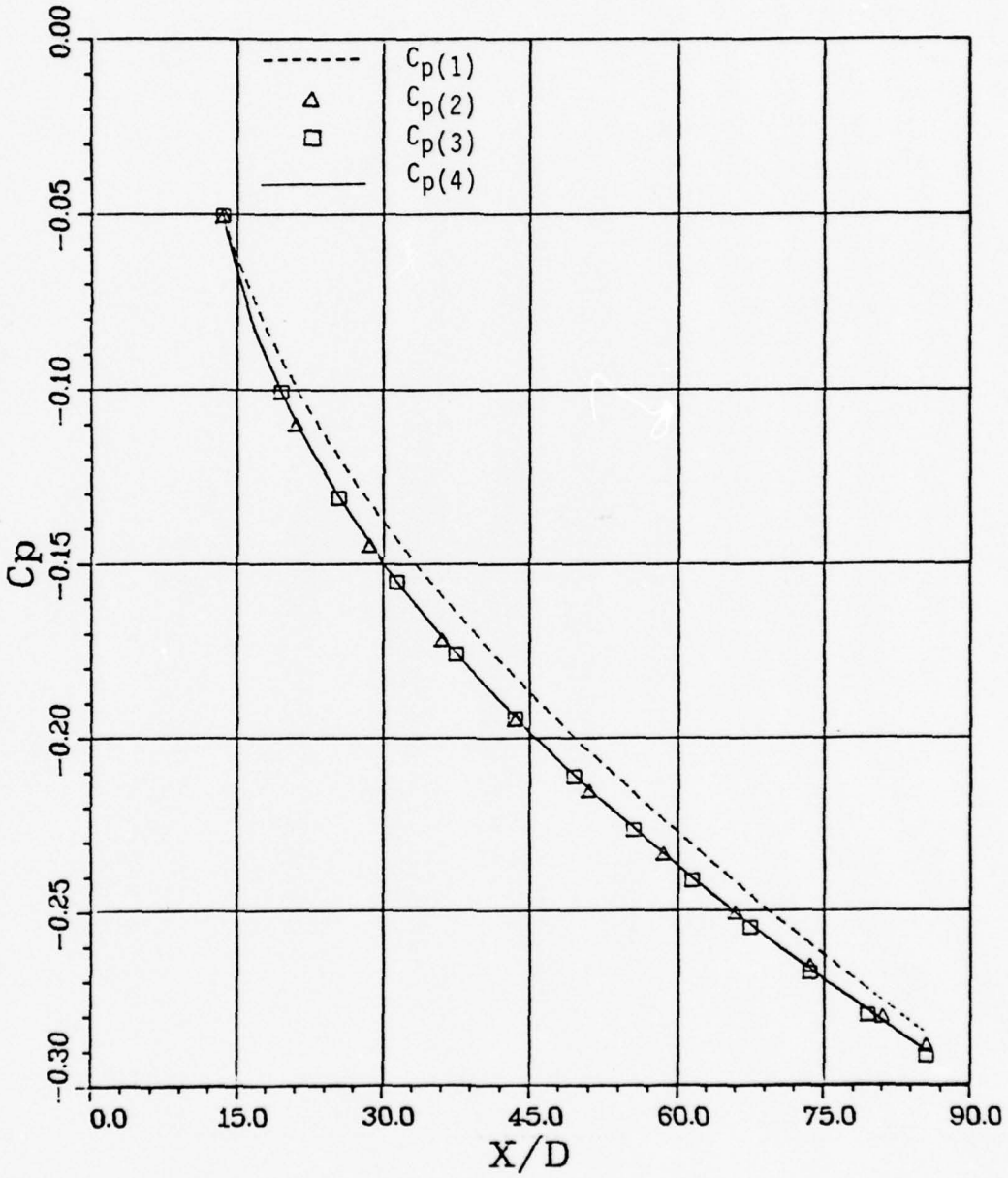

Figure 7. Convergence of C_p From the Iteration for $\Delta T = 0^oC$, $U_o = 2.06$ m/sec

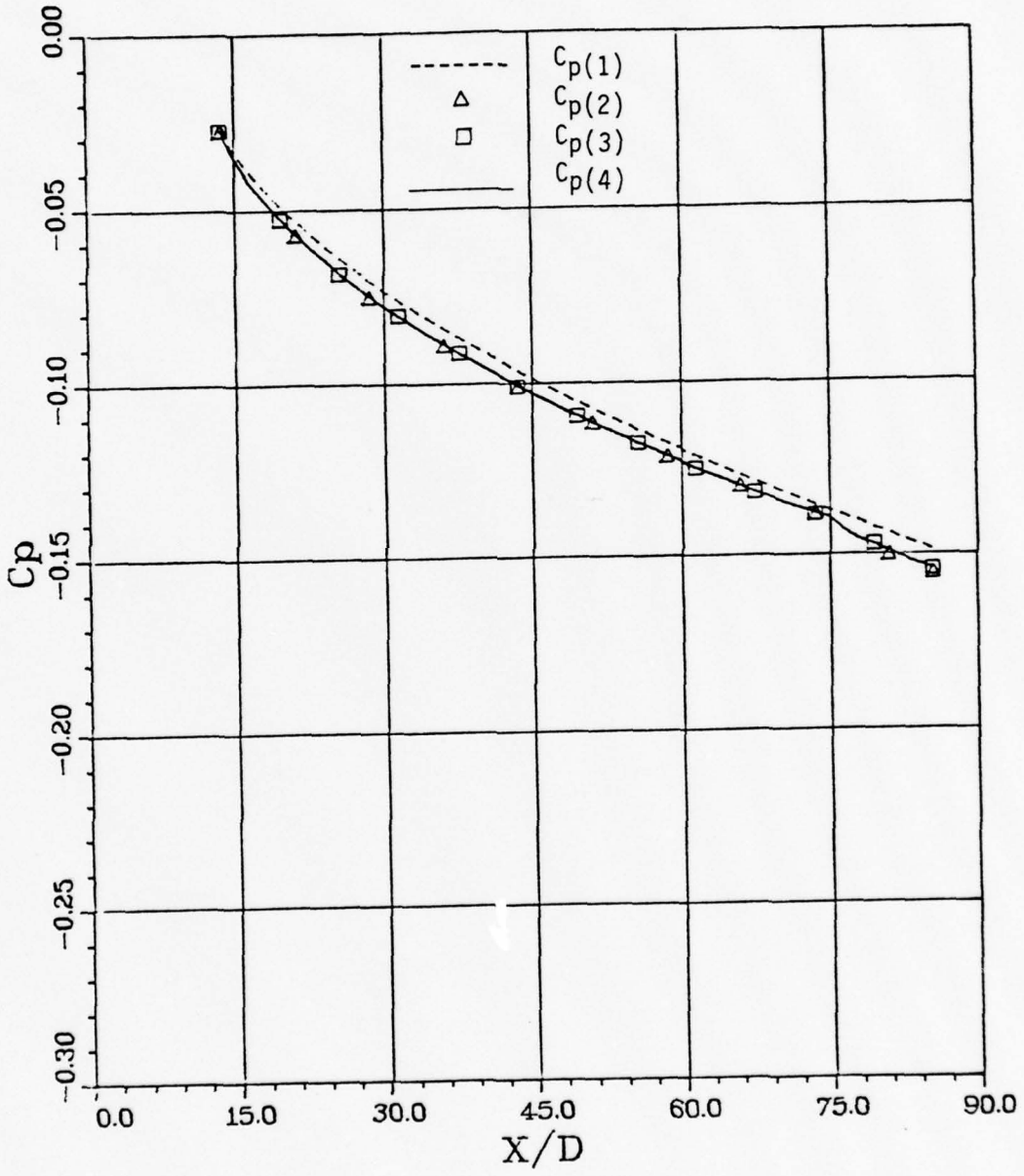

Figure 8. Convergence of C_p From the Iteration for $\Delta T = 8.33^{o}C$, $U_o = 6.89$ m/sec

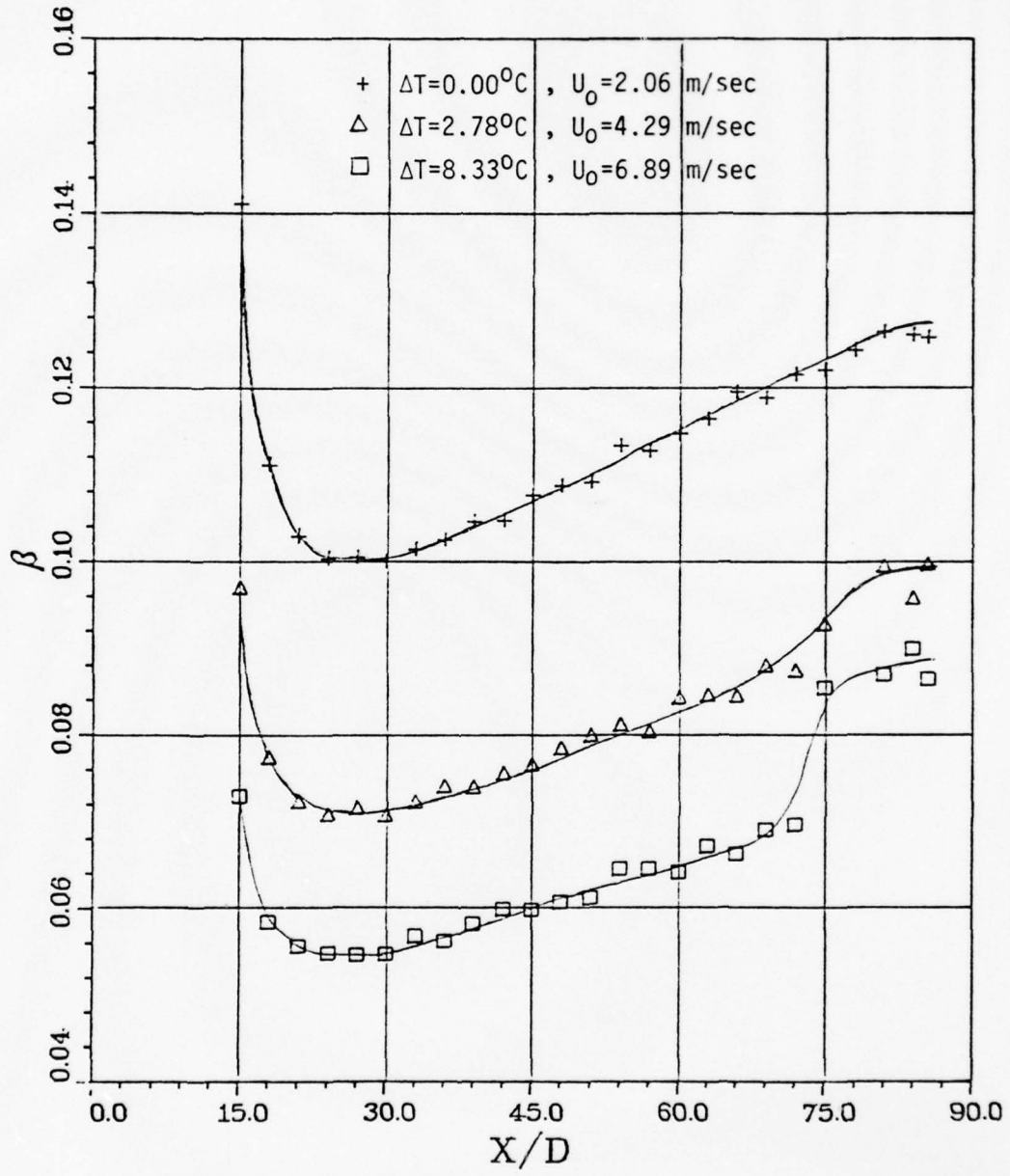

Figure 9. Variation of the Pressure Gradient Parameter ,β, in the Flow Tube

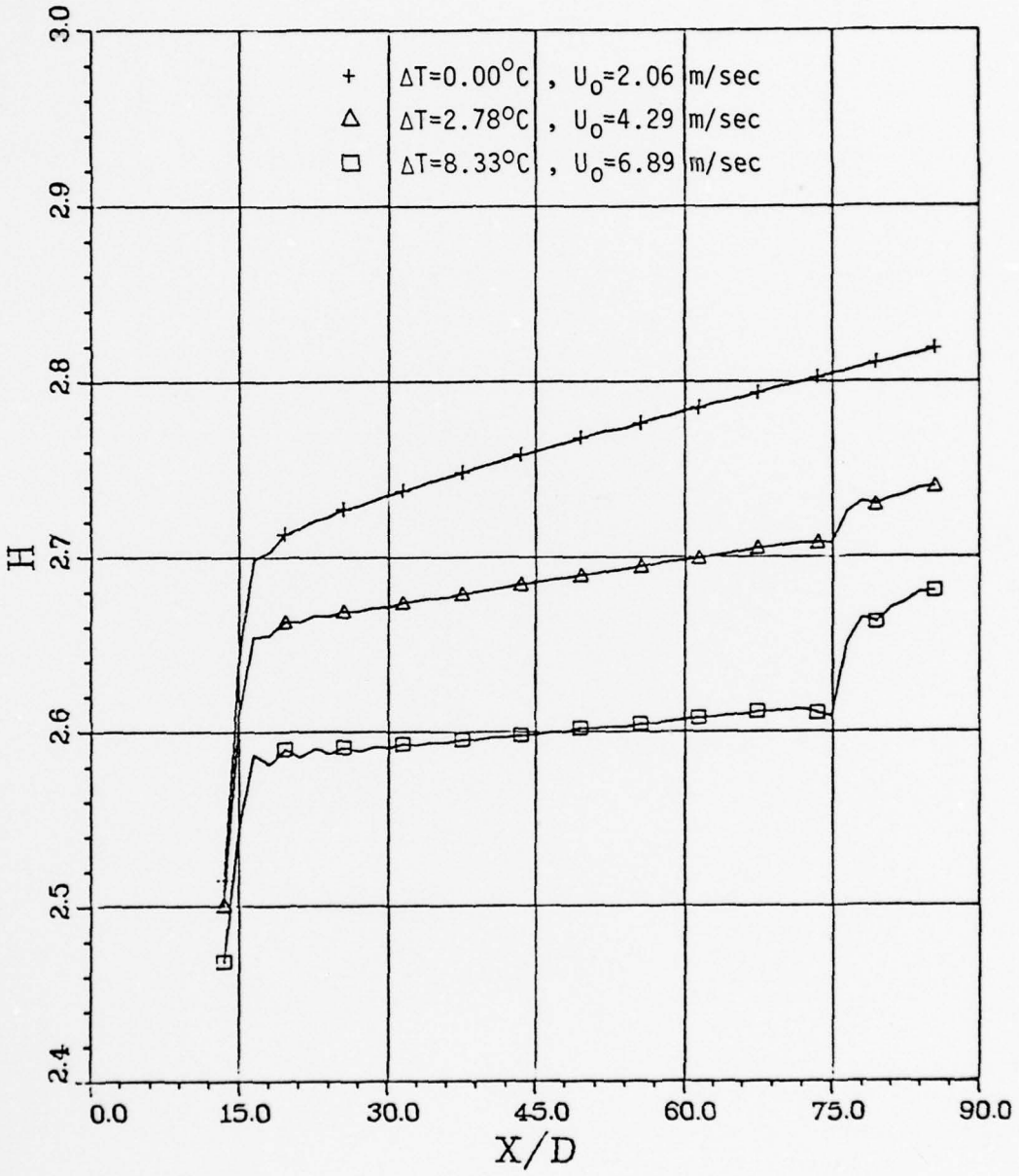

Figure 10. Variation of the Boundary-Layer Shape Factor ,H, in the Flow Tube

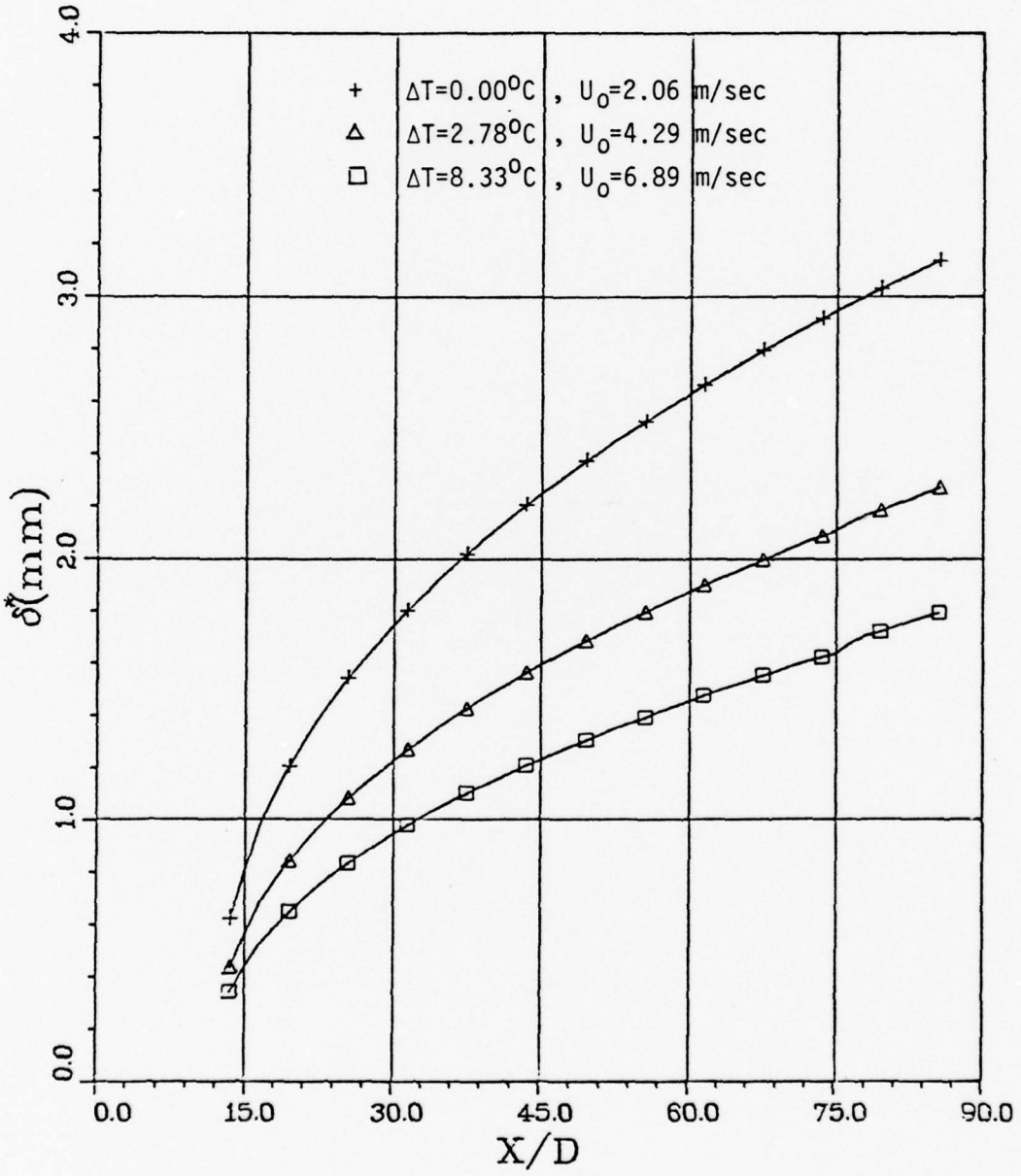

Figure 11. Variation of the Boundary-Layer Displacement Thickness, δ^*, in the Flow Tube

Figure 9 shows the variation of the pressure gradient parameter β (defined as $\beta = \frac{2\xi}{U_e}\frac{dU_e}{d\xi}$, where ξ is the transformed distance parameter, see Gentry & Wazzan, 1976) in the flow tube for various operating conditions. We note that the computed values of β depend strongly on the flow speed and increase considerably in the downstream direction. The flow in the tube is neither a zero pressure gradient flow ($\beta = 0$) nor a constant pressure gradient parameter flow. Hence analytical results based on either of those assumptions would not be strictly legitimate. It is also noted that parameter β has a sudden jump at the joint of heated and unheated sections.

Figure 10 shows the variations of shape factor H ($H = \delta^*/\theta$) in the flow tube. In the cases of heated flow conditions ($\Delta T = 2.78^oC$ and $\Delta T = 8.33^oC$), the shape factors increase considerably in the unheated extension tube, indicating the boundary-layer has become more unstable.

Figure 11 shows the variations of the displacement thickness in the flow tube for various flow conditions. As can be seen in the figure, a lower flow velocity has a higher displacement thickness and, in turn, has a much larger pressure gradient parameter β.

The boundary-layer stability analyses have been performed for the selected flow conditions. The computed spatial amplification factors for various disturbance frequencies are shown in Figures 12 to 15. A summary of the results is presented in Table 2.

At the experimental transition location, end of the flow tube with one extension, the corresponding amplification factors vary from $e^{11.6}$ to $e^{15.8}$ with a mean value of $e^{14.0}$. All of these amplification factors are much higher than the traditional "e^9" criterion which was proposed by Smith (Jaffe, 1969).

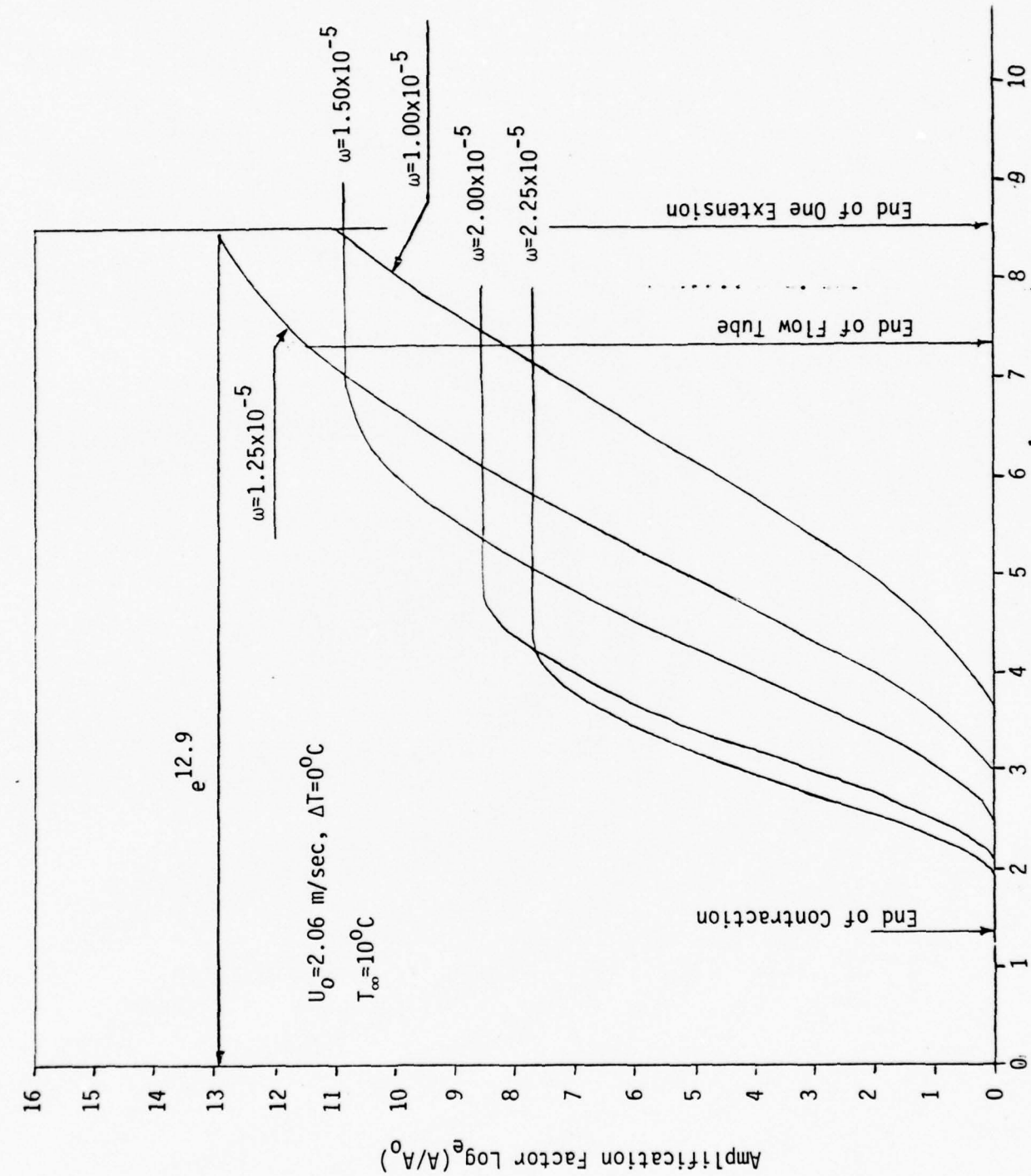

Figure 12. Spatial Amplification Factors in Boundary Layer for U_o=2.06 m/sec, $\Delta T=0^oC$, $T_\infty=10^oC$

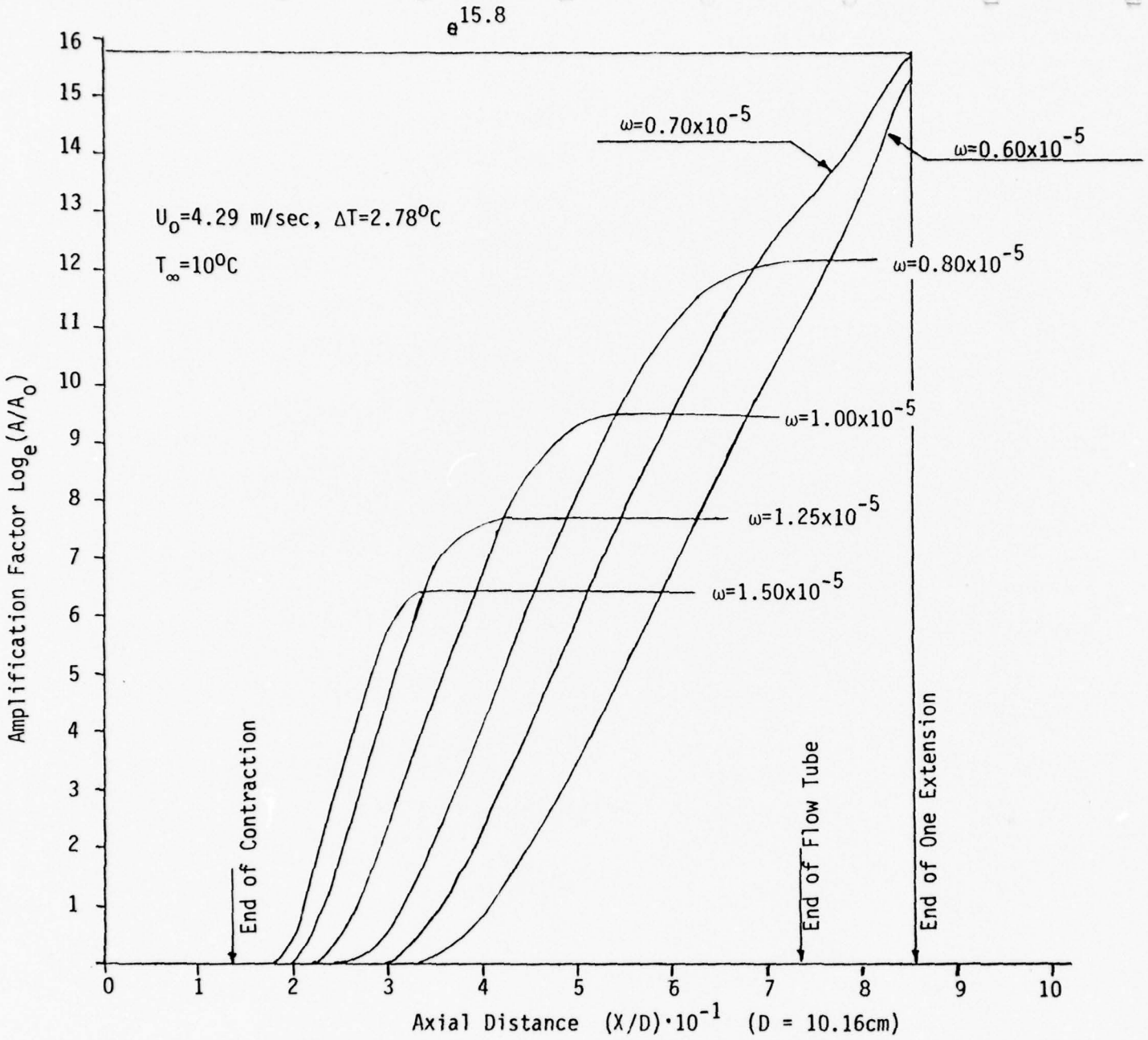

Figure 13. Spatial Amplification Factors in Boundary Layer for U_o=4.29 m/sec, ΔT=2.78°C, T_∞=10°C

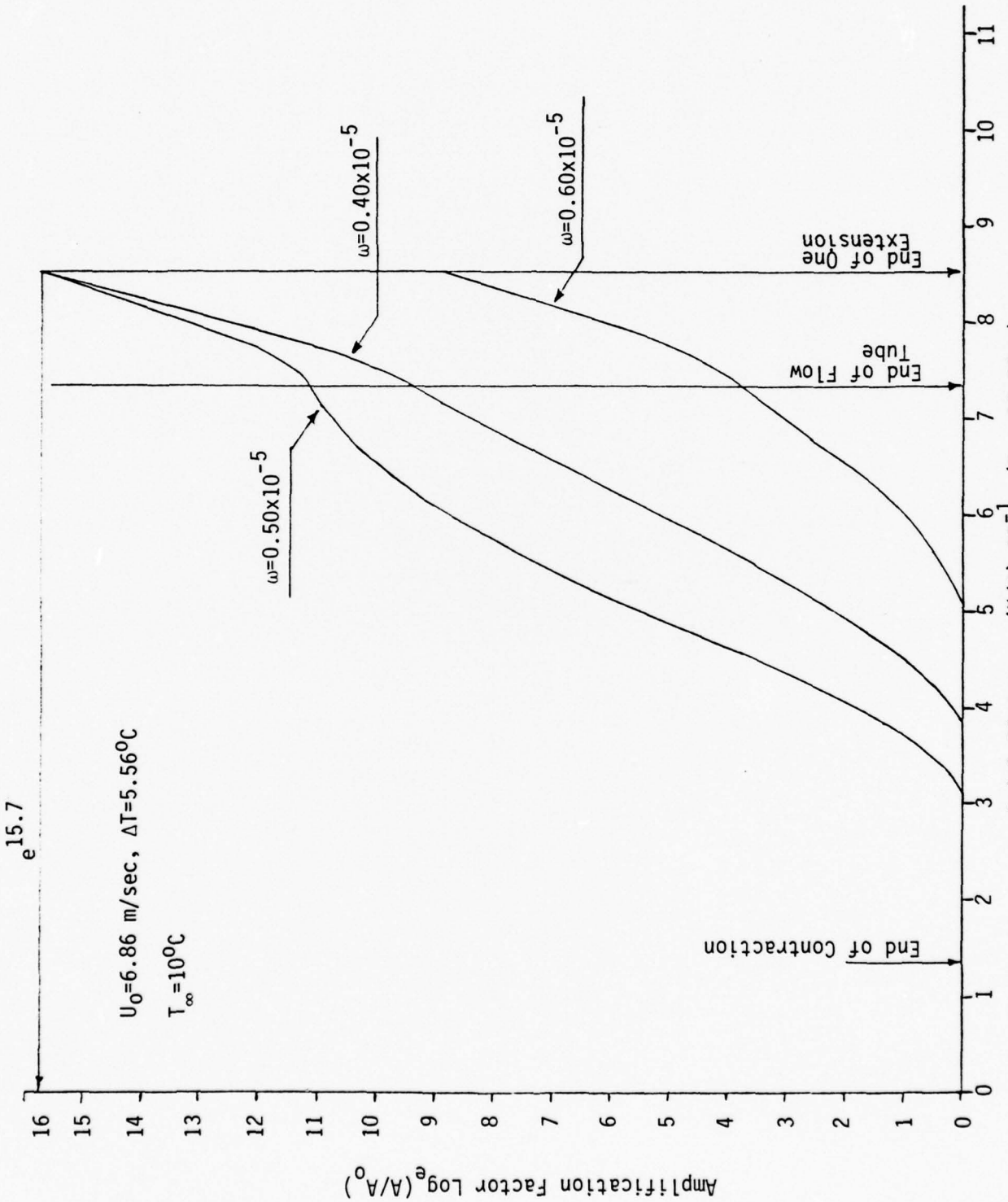

Figure 14. Spatial Amplification Factors in Boundary Layer for U_o=6.86 m/sec, ΔT=5.56°C, T_∞=10°C

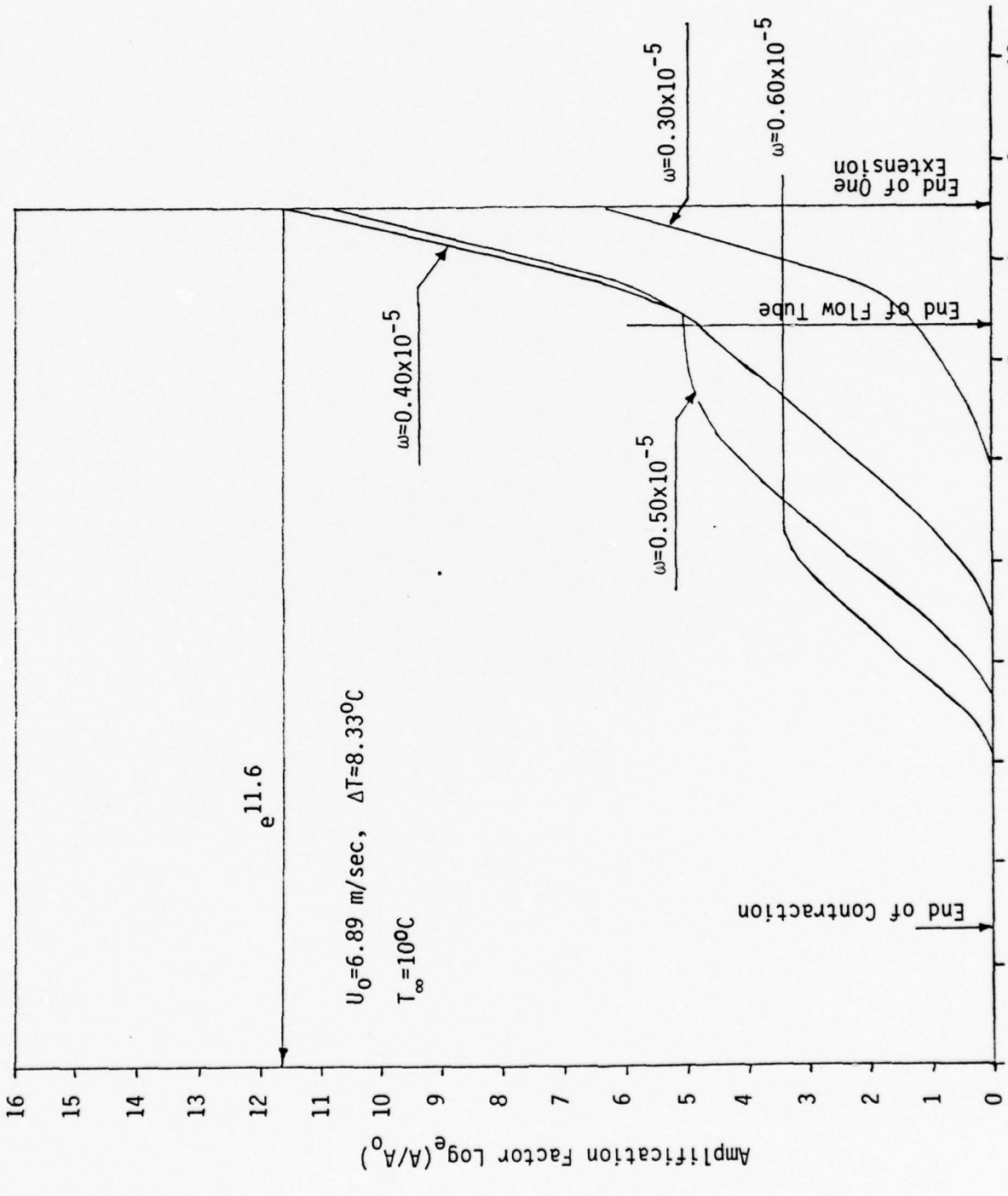

Figure 15. Spatial Amplification Factors in Boundary Layer for U_o=6.89 m/sec, ΔT=8.33°C, T_∞=10°C

TABLE 2

Amplification Factors At The End Of One Extension Tube

Non-Dimensional Frequency $\omega \times 10^5$	$\Delta T=0^oC$ $U_o=2.06m/sec$	$\Delta T=2.78^oC$ $U_o=4.29m/sec$	$\Delta T=5.56^oC$ $U_o=6.86m/sec$	$\Delta T=8.33^oC$ $U_o=6.89m/sec$
2.25	7.63			
2.00	8.50			
1.75	9.41			
1.50	10.83	6.43		
1.25	* 12.91	7.70	3.11	0.07
1.00	11.08	9.50	4.37	0.49
0.90	9.14	10.87	5.29	1.00
0.80	6.76	12.14	6.05	1.51
0.70	4.20	* 15.76	7.31	2.21
0.60		15.37	9.04	3.45
0.50		11.77	15.68	10.79
0.40		6.28	* 15.73	* 11.60
0.30		1.23	8.91	6.37
0.20				1.32

* The maximum value of the Amplification Factor.

In an attempt to establish the "e^n" criterion for the flow tube system, another set of the analytical calculation has been performed for flow conditions $\Delta T = 0^oC$ to 16.67^oC and $U_o = 1.83$ m/sec to 6.71 m/sec.

The computed spatial amplification factors for boundary-layer disturbances are shown in Figures 16 to 22. Three different criteria (namely, amplification ratios of e^9, e^{11}, and e^{14}) have been used to estimate where the boundary layer would undergo transition. A summary of these results is presented in Figure 23.

It is noted that the experimentally quoted transition Reynolds number is based on the assumption that the boundary layer begins at a virtual origin 30.5 cm upstream of the test section. In the present study, a more realistic assumption is made in that the boundary layer is assumed to begin at the upstream side of the contraction section. Therefore, the experimental data in Figure 23 have been corrected from those shown in Figure 1 by this difference in origin in order to compare with the analytical results.

In general, the analytical curves predict the same trend as the experimental data. For surface overheats, ΔT, less than 7^oC, the e^{14} curve appears to have a better agreement with the experimental data which leads to the same conclusion as the previous analytical results. Since the increases in transition Reynold's number in this flow tube facility have been achieved by increasing the flow velocity while the basic geometrical parameters of the facility remain the same, the limitation of the "maximum" achievable Reynold's number in the flow tube may also be a result of increasing freestream disturbance level as the flow velocity increases (a unit Reynold's number effect). This conjecture needs to be further substantiated or reputed in the future.

It is also of interest to note that the unstable range of Tollmien-Schlichting waves with the flow-tube boundary layer is in the low frequency region, ranging from 5Hz to 25Hz.

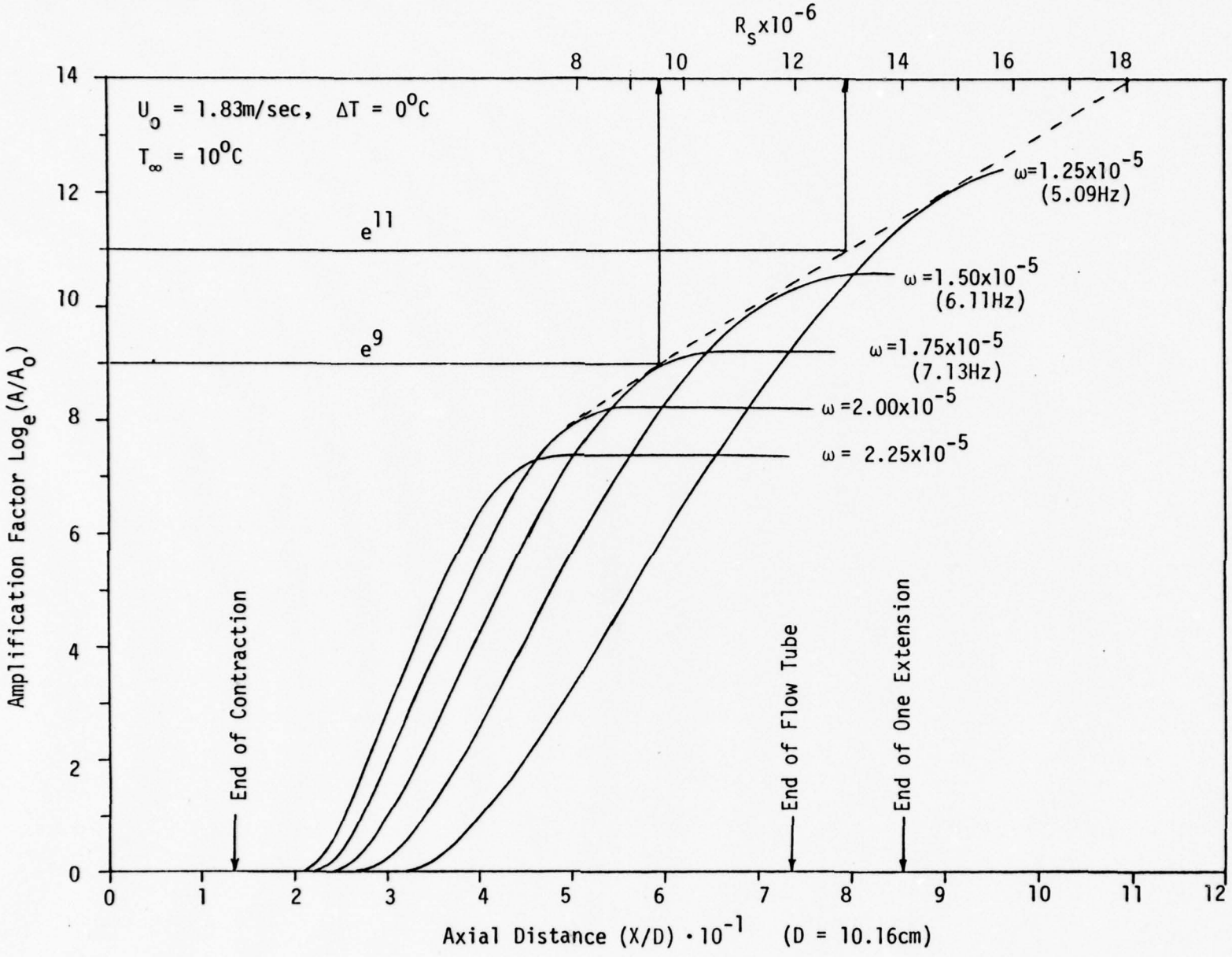

Figure 16. Spatial Amplification Factors in Boundary Layer for U_o=1.83m/sec, $\Delta T = 0^oC$, $T_\infty = 10^oC$

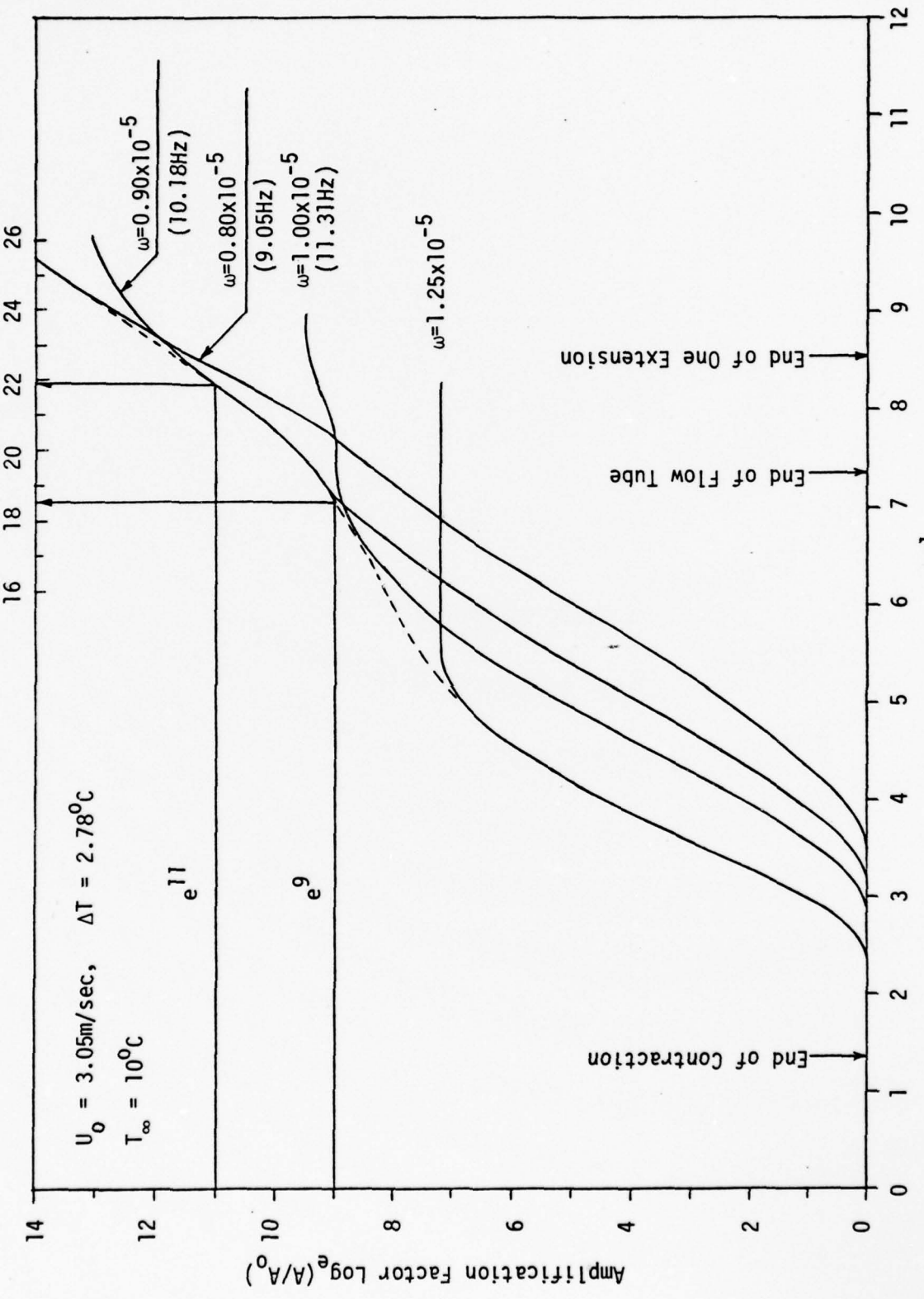

Figure 17. Spatial Amplification Factors in Boundary Layer for U_o=3.05m/sec, ΔT = 2.78^oC, T_∞ = 10^oC

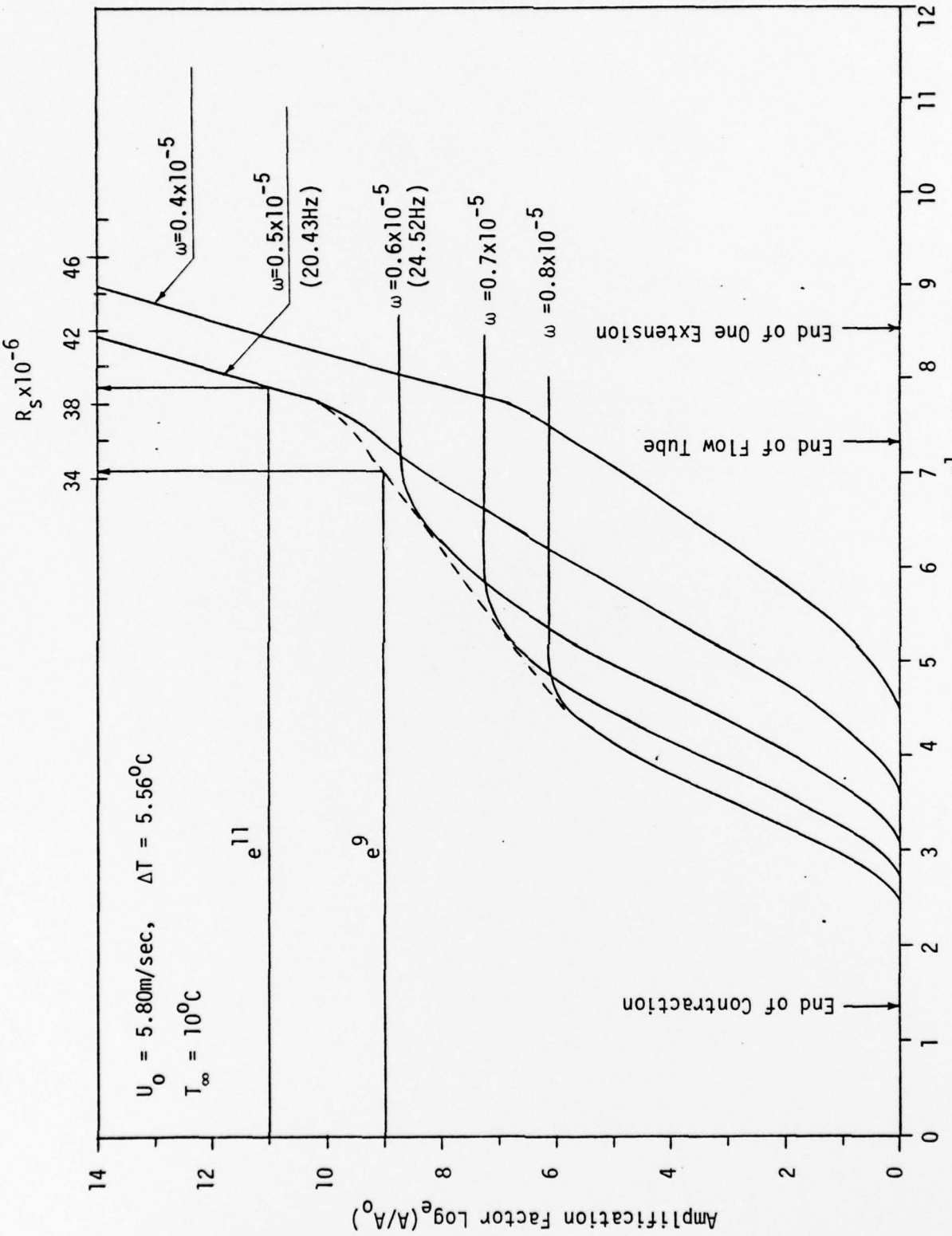

Figure 18. Spatial Amplification Factors in Boundary Layer for U_o=5.80m/sec, ΔT = 5.56^oC, T_∞ = 10^oC

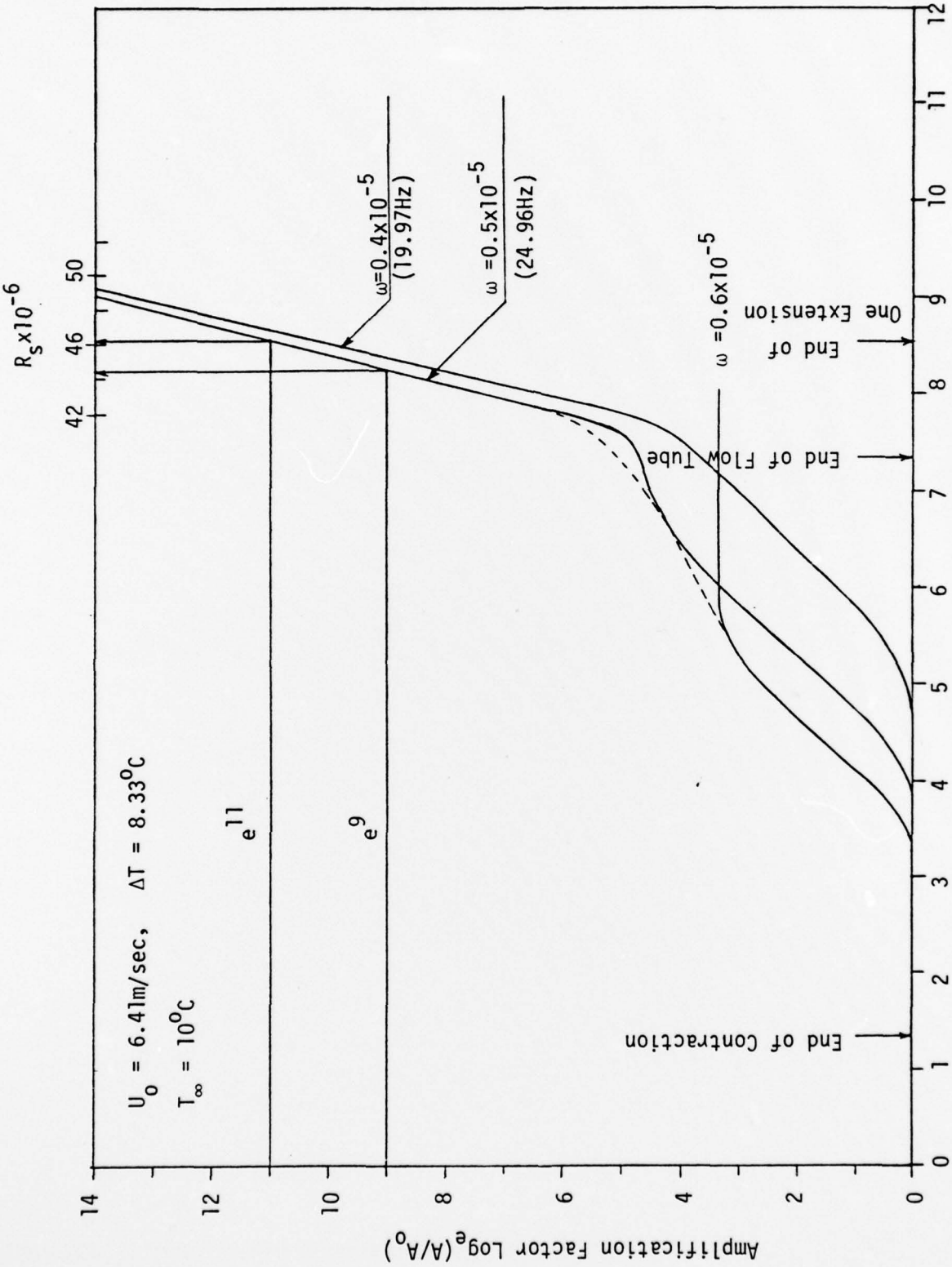

Figure 19. Spatial Amplification Factors in Boundary Layer for U_o=6.41m/sec, $\Delta T = 8.33^oC$, $T_\infty = 10^oC$

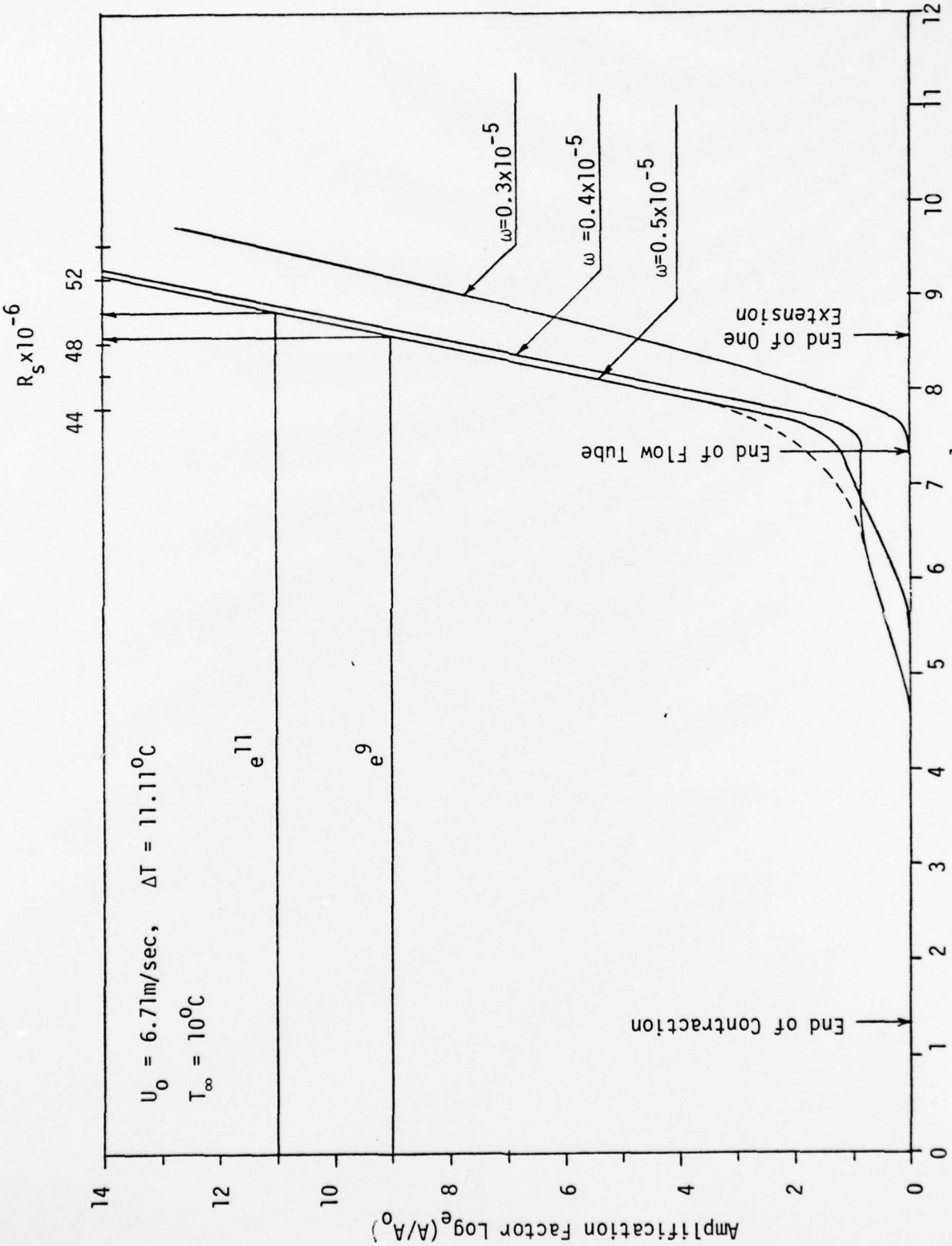

Figure 20. Spatial Amplification Factors in Boundary Layer for U_o=6.71m/sec, ΔT = 11.11^oC, T_∞ = 10^oC

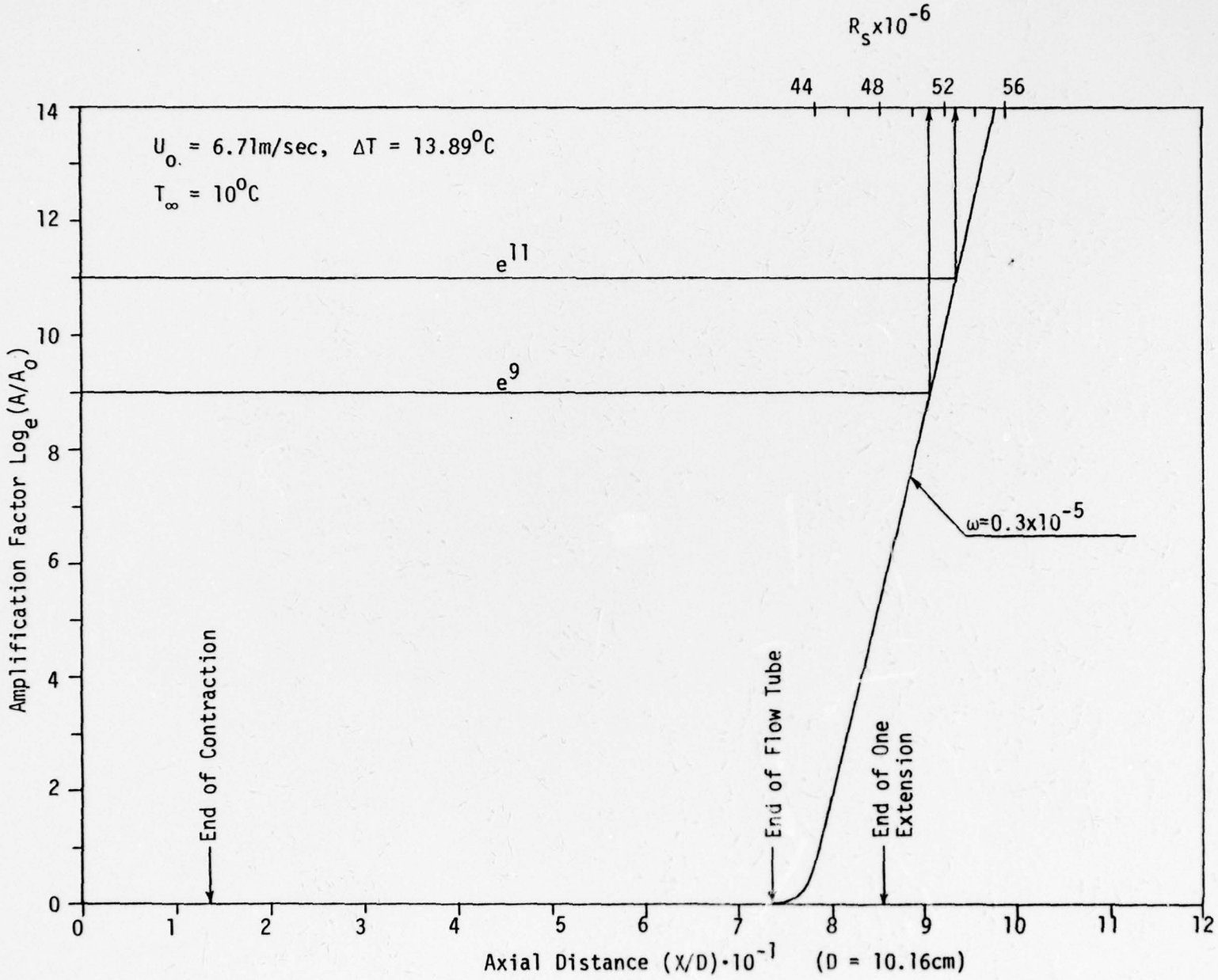

Figure 21. Spatial Amplification Factors in Boundary Layer for U_o=6.71m/sec, ΔT = 13.89°C, T_∞ = 10°C

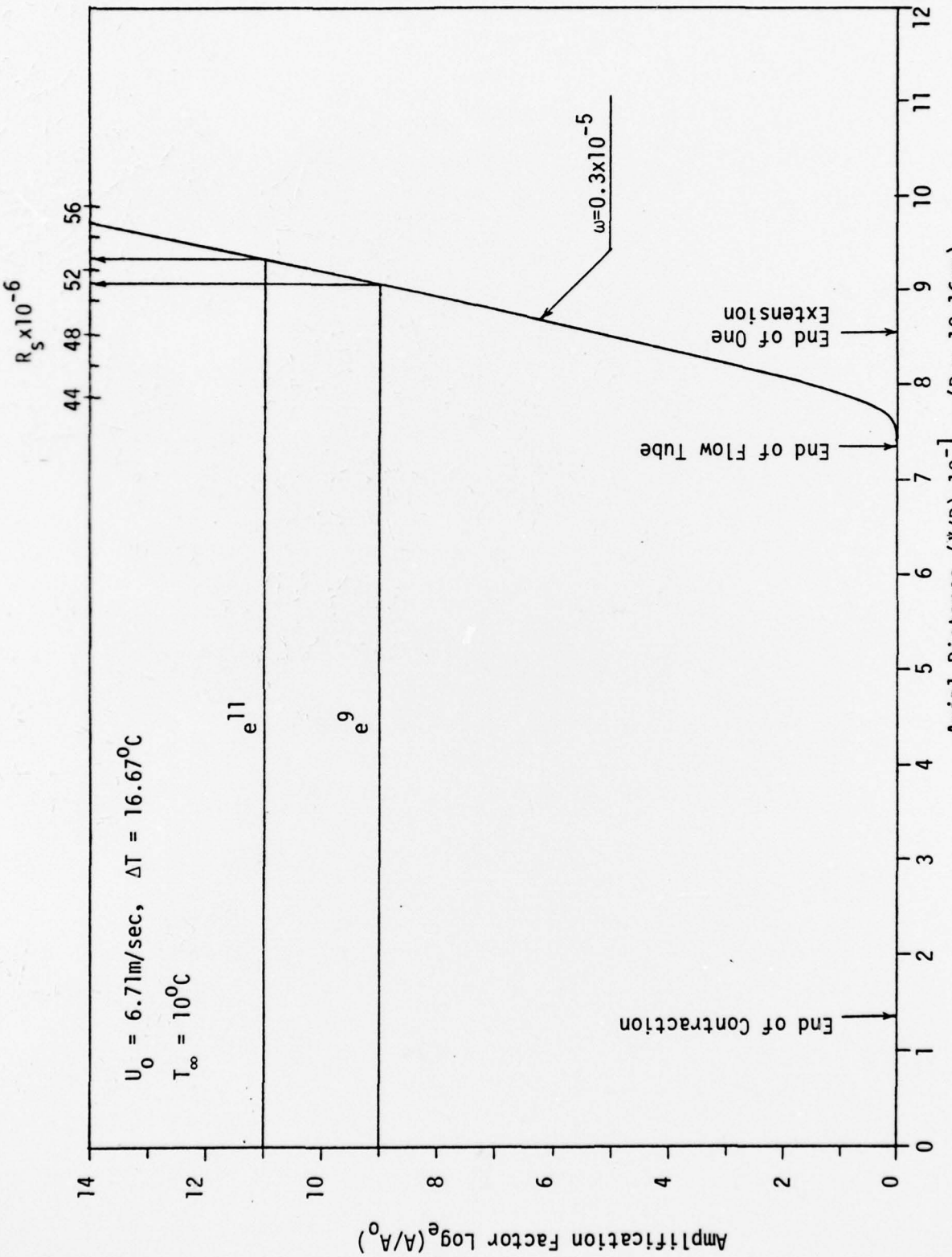

Figure 22. Spatial Amplification Factors in Boundary Layer for U_o=6.71m/sec, ΔT = 16.67°C, T_∞ = 10°C

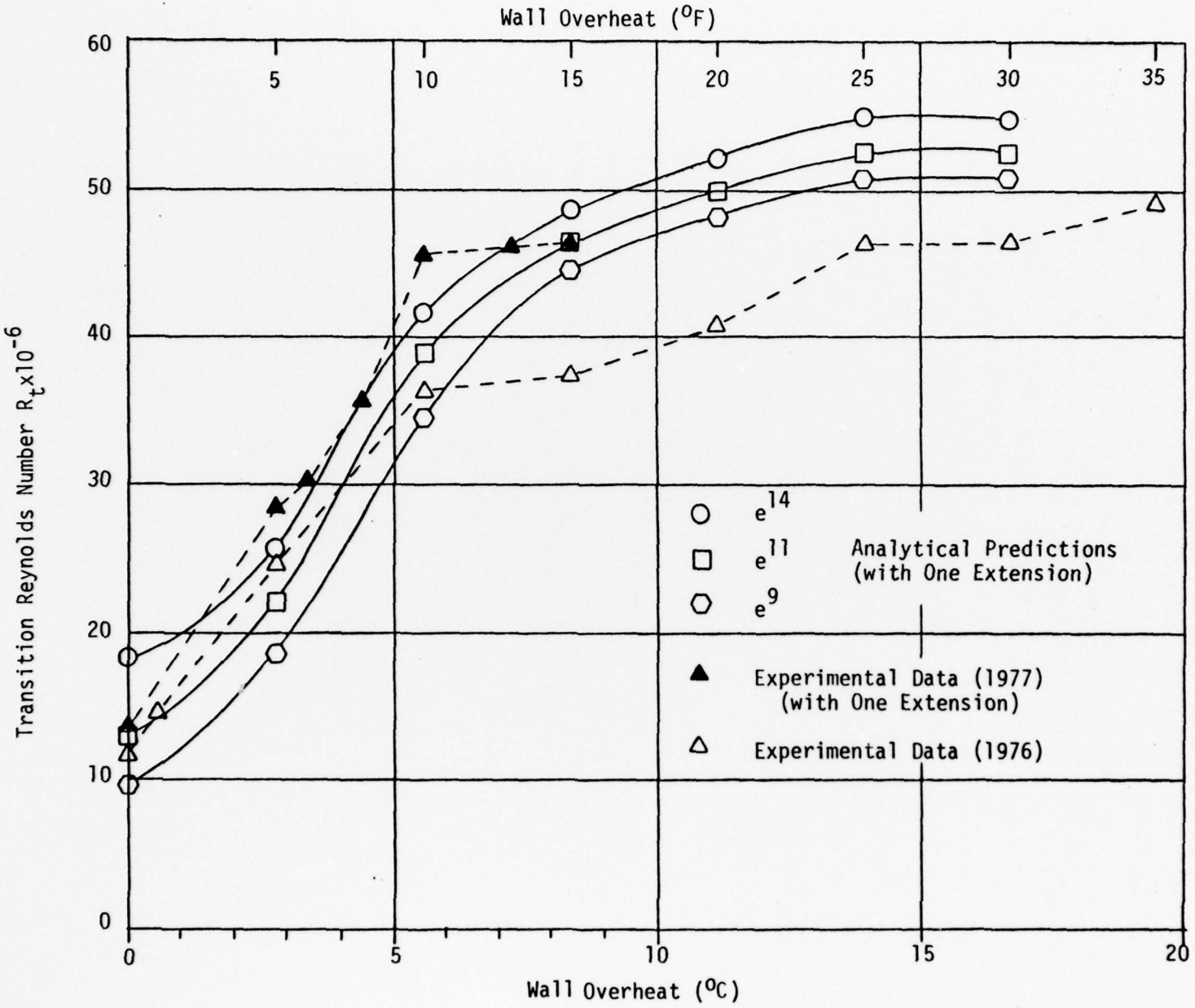

Figure 23. Comparison Between Experimental and Analytical Boundary-Layer Transition Results

The dependence of the transition Reynolds number at large surface overheat may be better understood by a close examination of the spatial amplification results for various surface overheat conditions (Figure 16 to 22). These results show that the contribution to the amplification factor in the unheated section becomes more important as ΔT increases. Based on the e^{14} criterion, the percentage contribution from both the heated and unheated portions of the flow tube are presented in the following table.

Surface Overheat ΔT (^{o}C)	Percentage Amplification from Heated Tube	Percentage Amplification from Unheated Tube
0.00	74	26
2.78	66	34
5.56	64	36
8.33	34	66
11.11	9	91
13.89	0	100
16.67	0	100

We note that the effectiveness of surface heating reduces to zero beyond $12^{o}C$. To illustrate the improvement in transition Reynolds number which might be realized if the extension tube were heated, calculations were performed by assuming the same surface overheat in the extension tube. The computed amplification ratios for $\Delta T = 5.56^{o}C$ and $\Delta T = 8.33^{o}C$ are shown in Figures 24 and 25, respectively. As shown in the table below, at the end of the extension tube, as much as a 45% decrease in amplification factor may have been achieved when $\Delta T = 8.33^{o}C$. Therefore, a significant improvement of the experimental performance in the tube test may be expected by heating the extension tube.

Surface Overheat ΔT (^{o}C)	Freestream Speed U_o (m/sec)	At End of One Extension Tube X/D = 85.5	
		$Log_e(A/A_o)$ with Unheated Ext. Tube	$Log_e(A/A_o)$ with Heated Ext. Tube
5.56	5.80	14.2	10.8
8.33	6.41	10.8	5.9

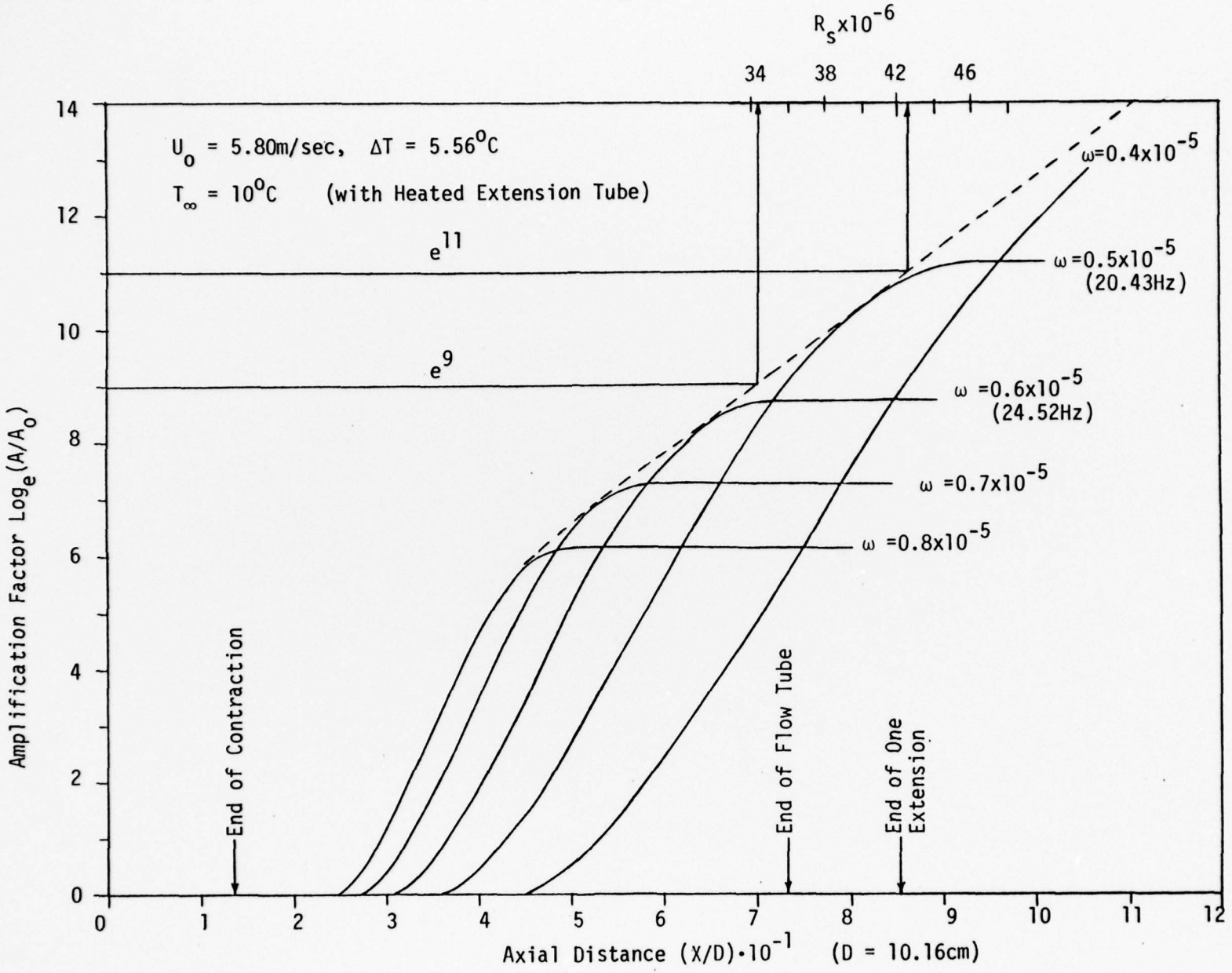

Figure 24. Spatial Amplification Factors in Boundary Layer for U_o=5.80m/sec, ΔT = 5.56°C, T_∞ = 10°C (with Heated Extension Tube)

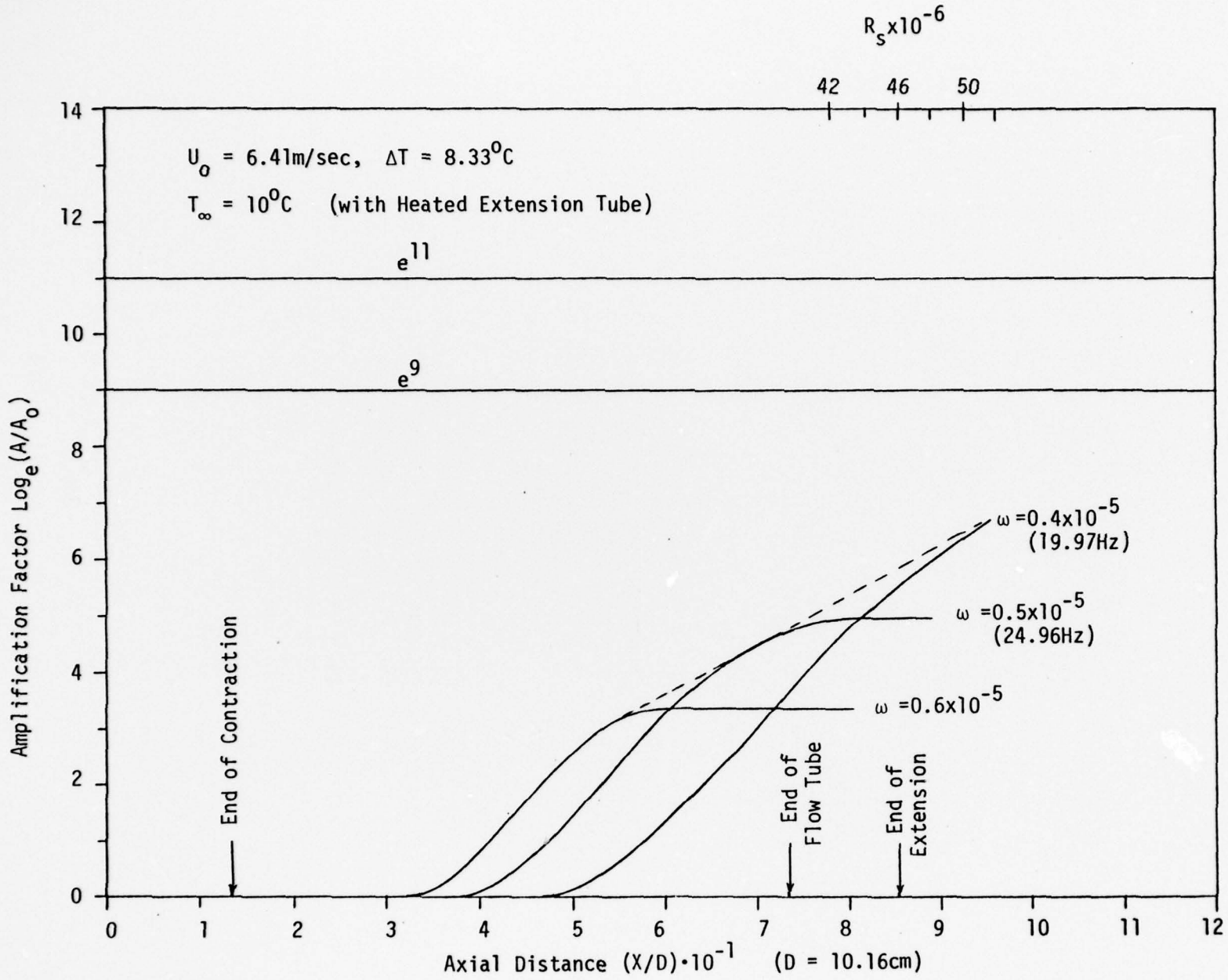

Figure 25. Spatial Amplification Factors in Boundary Layer for U_o=6.41m/sec, ΔT = 8.33°C, T_∞ = 10°C (with Heated Extension Tube)

4. SUMMARY AND CONCLUSIONS

This report documents a complementary analytical study to the Colorado flow-tube experiment. The main conclusions are:

- An improved analytical method for analyzing boundary-layer transition in the flow tube has been developed. The method includes the effects of transverse curvature and upstream contraction on the boundary-layer development, coupled with an iterative technique to account for the displacement thickness correction to the pressure distribution in the flow tube.

- A series of calculations has been performed to simulate the flow-tube experiment, a heated test section with one unheated section. At the experimental transition location, the computed amplification factors vary from $e^{11.6}$ to $e^{15.8}$ with a mean value of $e^{14.0}$ which is much higher than the traditional "e^9" criterion.

- Based on the "e^{14}" criterion, reasonably favorable comparisons with the experimental results are obtained with this more accurate computation scheme. The calculations provide the explanation, at least partially, of the apparent reduced effectiveness of surface heating at large ΔT. The explanation rests upon the role of the unheated section and the effects unique to a tube boundary layer.

- Further calculations indicate that a significant improvement of the tube performance may be obtained by heating of the extension tube. These results, however, do not explain the experimental findings of Barker. Bear in mind that this report only covers the analytical study dealing with main features unique to a flow tube. Several other features which might limit the transition Reynold's number in a flow tube, such as the effects of free stream turbulence, unsteadiness of the mean flow, buoyancy forces, surface roughness, surface waviness, suspended particulate, or the influence of downstream exit conditions are not included in this study.

ACKNOWLEDGEMENT

The author would like to express his appreciation to Dr. D. R. S. Ko of DynaTech for his helpful assistance in the preparation of this report. Sincerest appreciation is also extended to Dr. P. A. Selwyn of DARPA, Dr. S. J. Barker of Poseidon Research, Dr. E. Reshotko of Case Western Reserve University, Dr. R. L. Gran, Mr. W. W. Haigh, and Mr. A. M. O. Smith of DynaTech for their invaluable comments and suggestions.

REFERENCES

Autonetics Group, "Results of the Twenty Foot Heated Flow Tube Experiment", Rockwell International Report C76-1629/201, December 1976.

Barker, S.J., Jennings, C., "The Effect of Wall Heating Upon Transition in Water Boundary Layers", AIAA Paper, 1977.

Barker, S.J., "Transition in Heated-Wall Boundary Layers in a Tube: The Effect of Contamination, Downstream Boundary Conditions and Buoyancy", Poseidon Research Report No. 15, April, 1978.

Gentry, A.E., "The Transition Analysis Program System, Volume 1 -- User's Manual", McDonnell Douglas Report No. MDC J7255/01, 1976.

Gentry, A.E., and Wazzan, A.R., "The Transition Analysis Program System, Volume II -- Program Formulation and Listings", McDonnell Douglas Report No. MDC J7255/02, 1976.

Jaffe, N.A., Okamura, T.T., and Smith, A.M.O., "The Determination of Spatial Amplification Factors and Their Application to Predicting Transition", AIAA Paper No. 69-10, January 1969.

Tzou, K.T.S. Smith, A.M.O., Kubota, T., Haigh, W.W., "Comparison of Relative Location of Transition in the Flow Tube Experiment with Its Location on the Corresponding Axisymmetric Body", Dynamics Technology Report DT-7610-2, November 1977.

Wazzan, A.R., Okamura, T.T., and Smith, A.M.O., "The Stability of Water Flow Over Heated and Cooled Flat Plates", Trans. ASME 90, Series C, 1968.

Wazzan, A.R., Okamura, T.T., and Smith, A.M.O., "The Stability and Transition of Heated and Cooled Incompressible Laminar Boundary Layers", Proc. 4th International Heat Transfer Conference, Paris, 1970.

DISTRIBUTION LIST FOR UNCLASSIFIED
TECHNICAL REPORTS ISSUED UNDER
CONTRACT N00014-77-C-0005 TASK NR 062-562

All addresses receive one copy unless otherwise specified.

Defense Documentation Center
Cameron Station
Alexandria, VA 22314 12 copies

Technical Library
David W. Taylor Naval Ship
Research and Development Center
Annapolis Laboratory
Annapolis, MD 21402

Library
Naval Academy
Annapolis, MD 21402

Dr. Philip A. Selwyn
DARPA/TTO
1400 Wilson Boulevard
Arlington, VA 22209

Office of Naval Research
Code 1021P (ONRL)
800 N. Quincy Street
Arlington, VA 22217 6 copies

Office of Naval Research
Code 211
800 N. Quincy Street
Arlington, VA 22217

Office of Naval Research
Code 438
800 N. Quincy Street
Arlington, VA 22217 3 copies

NASA Scientific and Technical
Information Facility
P. O. Box 8757
Baltimore/Washington Inter-
national Airport
Maryland 21240

Dr. Steven J. Barker
Poseidon Research
11777 San Vicente Boulevard
Los Angeles, CA 90049

Librarian
University of California
Dept. of Naval Architecture
Berkeley, CA 94720

Library (Code 5641)
Dr. W. E. Cummins, Code 15
Dr. J. H. McCarthy, Code 1552
David W. Taylor Naval Ship Research
and Development Center
Bethesda, MD 20084 3 copies

Professor P. Leehey
Massachusetts Institute of Technology
Department of Ocean Engineering
Cambridge, MA 02139

Library
Naval Weapons Center
China Lake, CA 93555

Professor E. Reshotko
Case Western Reserve University
Div. of Chemical Engineering Science
Cleveland, OH 44106

Technical Library
Naval Weapons Surface Center
Dahlgren Laboratory
Dahlgren, VA 22418

Mr. Dennis Bushnell
NASA Langley Research Center
Langley Station
Hampton, VA 23365

Professor L. Landweber
Institute of Hydraulic Research
University of Iowa
Iowa City, IA 52242

Mr. Carl G. Jennings
Rockwell International Corp.
Autonetics Group
Anaheim, CA 92803

Distribution List (Cont.)

Fenton Kennedy Document Library
The Johns Hopkins University
Applied Physics Laboratory
Johns Hopkins Road
Laurel, MD 20810

Dr. S. Orszag
Cambridge Hydrodynamics, Inc.
54 Baskin Road
Lexington, MA 02173

Professor Tuncer Cebeci
California State University
Mechanical Engineering Dept.
Long Beach, CA 90840

Dr. T. D. Taylor
The Aerospace Corporation
P. O. Box 92957
Los Angeles, CA 90009

Lorenz G. Straub Library
St.Anthony Falls Hydraulic Lab.
University of Minnesota
Minneapolis, MN 55414

Library
Naval Postgraduate School
Monterey, CA 93940

Technical Library
Mr. Fred White, Code 36301
Mr. Richard Nadolink, Code 3635
Naval Underwater Systems Center
Newport, RI 02840 3 copies

Professor H. W. Liepmann
Graduate Aeronautical Laboratories
California Institute of Technology
Pasadena, CA 91109

Dr. Leslie M. Mack
Jet Propulsion Laboratory
California Institute of Technology
Pasadena, CA 91125

Mr. Roy Gulino
Westinghouse Electric Corp.
Oceanic Division
Box 1488
Annapolis, MD 21404

Technical Library
Dr. George L. Donohue, Code 6302
Dr. Michael M. Reischman, Code 6342
Dr. James Logan, Code 631
Naval Ocean Systems Center
San Diego, CA 92132 4 copies

Dr. Carl Gazley, Jr.
The Rand Corporation
1700 Main Street
Santa Monica, CA 90406

Librarian
Naval Surface Weapons Center
White Oak Laboratory
Silver Spring, MD 20910

Dr. D. R. S. Ko
Dynamics Technology, Inc.
3838 Carson Street, Suite 110
Torrance, CA 90503

Dr. Phillip S. Klebanoff
National Bureau of Standards
Mechanics Division
Washington, DC 20034

Dr. Robert J. Hansen
Naval Research Laboratory
Code 2627
Washington, DC 20375

Library (Code 09GS)
Dr. E. G. Liszka, Code 03421
Dr. Thomas E. Pierce, Code 03512
Mr. R. Manning, Code 395A
Naval Sea Systems Command
Washington, DC 20362 4 copies

Professor Blaine R. Parkin
Dr. G. C. Lauchle
Pennsylvania State University
Applied Research Laboratory
University Park, PA 16802 2 copies